

Solubility and In-vitro Drug Permeation Behaviour of Ethenzamide Cocrystals Regulated at Physiological pH Environments

Rajiv Khatioda, Basanta Saikia, Pranab Jyoti Das and Bipul Sarma*

Department of Chemical Sciences, Tezpur University, Napaam-784028, Assam, India

E-mail: sarmabipul@gmail.com, bcsarma@tezu.ernet.in

INDEX

Table S1 Synthesis of ethenzamide (ZMD) cocrystals (**1** to **4**).

Fig. S1 FT-IR spectra of ZMD and its cocrystals (**1** to **4**).

Table S2 DSC melting onset of cocrystals **1** to **4**.

Fig. S2 TGA trace of **4** revealing release of inclusion solvent.

Fig. S3 Experimental PXRD pattern laid over simulated pattern from single crystal structure.

Table S3 Hydrogen bond parameters for cocrystals **1** to **4**

Fig. S4 Hirshfeld surface interaction in cocrystals **1** to **4**.

Fig. S5 Hirshfeld 2D finger print plots of interactions in cocrystals **1** to **4**.

Table S4 Cambridge Structural Database (CSD) analysis for various synthons.

Table S5 Dihedral angle of amide group in ZMD and its cocrystal systems.

Fig. S6 Stack plots of PXRD pattern of slurry experiment of **1** and **3** attributing phase stability of materials in aqueous medium.

Fig. S7 Stack plots of PXRD pattern of slurry experiment of **1** to **4** attributing phase stability of materials at pH 1.2 and 7.4 buffer medium.

Table S6 (a) Solubility of ZMD and its cocrystals (**1** to **4**) at different conditions. **(b)** Procedure of particle size distribution with plots for ZMD, cocrystal **1** & **3**.

Fig. S8 UV spectra of ZMD and its cocrystals (**1** to **4**) at different conditions.

Table S7 Wavelength value corresponding to the absorbance considered in calculating solubility and permeability parameters.

Fig. S9 Calibration curves for solubility determination.

Table S8 Permeability rate % at pH 1.2 and 7.4 in three set of experiments.

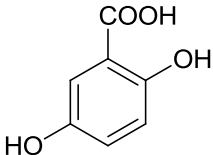
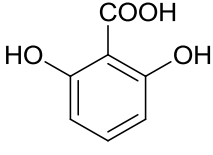
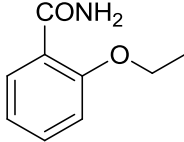
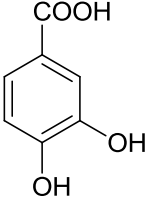
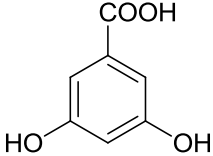
Fig. S10 Drug release at pH 1.2 and 7.4 at definite time period.

Fig. S11 ORTEP of cocrystals **1** to **4**.

Cocrystal Preparation

A mixture of ZMD and a coformer in 1:1 molar ratio was taken in a mortar and grinded manually using liquid assisted grinding (LAG) technique. The powder mixture was further dissolved in common laboratory solvents and kept for crystallization at ambient temperature (Table S1). The suitable crystals obtained after few days were further subjected to characterization using thermal, microscopic, spectroscopic and X-ray diffraction techniques.

Table S1. Synthesis of ZMD cocrystals with dihydroxybenzoic acid cofomers

Drug	Coformer	Crystallization solvent	Cocrystal	Stoichiometry/ solvent
		Toluene + Ethyl acetate	1	2:2
		Methanol	2	1:1
 Ethenzamide (API)		Toluene + Acetonitrile	3	1:1
		Methanol + Chloroform	4	1:3/ 2 H ₂ O

FT-IR Analysis

The IR spectrum of ZMD and multicomponent systems were recorded separately in Perkin Elmer Spectrophotometer using the KBr pellets ranging from 450 to 4000 cm^{-1} and are furnished below.

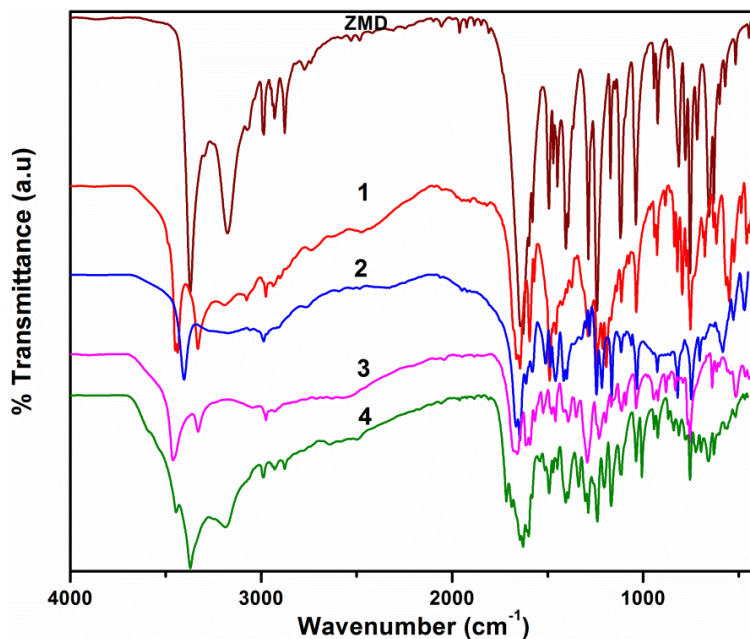


Fig. S1 FT-IR spectra of ZMD and its cocrystals **1** to **4**.

The major stretching frequencies (cm^{-1}) of cocrystals are:-

1: 1193 ($\text{C-O}_{\text{ether}}$), 1240 (C-O_{acid}), 1645 ($\text{C=O}_{\text{amide}}$), 1662 (C=O_{acid}), 3192 ($\text{N-H}_{\text{symmetric}}$), 3331 ($\text{N-H}_{\text{asymmetric}}$); 3437 (O-H); **2:** 1165 ($\text{C-O}_{\text{ether}}$); 1244 (C-O_{acid}), 1645 ($\text{C=O}_{\text{amide}}$), 1665 (C=O_{acid}), 2986 ($\text{N-H}_{\text{symmetric}}$); 3403 (O-H); **3:** 1166 ($\text{C-O}_{\text{ether}}$), 1292 (C-O_{acid}), 1643 ($\text{C=O}_{\text{amide}}$), 1659 (C=O_{acid}), 3330 ($\text{N-H}_{\text{asymmetric}}$), 3462 (O-H); **4:** 1167 ($\text{C-O}_{\text{ether}}$), 1239 (C-O_{acid}), 1599 ($\text{C=O}_{\text{amide}}$), 1628 (C=O_{acid}), 3371 ($\text{N-H}_{\text{asymmetric}}$), 3445 (O-H).

Table S2. DSC melting onset of cocrystals **1** to **4**.

Drug	Coformer	Coformer melting point (°C)	Cocrystals	Solvent loss temperature (°C)		Cocrystals melting point (°C)	
				Onset	Endset	Onset	Endset
ZMD [m.p.= 128-134]	2,5-DHBA	200-205	1	-	-	97.4	102.9
	2,6-DHBA	165	2	-	-	133.8	138.1
	3,4-DHBA	202-204	3	-	-	139.5	142.4
	3,5-DHBA	235-238	4	92.8	102.2	137.1	141.0

Fig. S2 TGA trace of **4** revealing release of inclusion solvent.

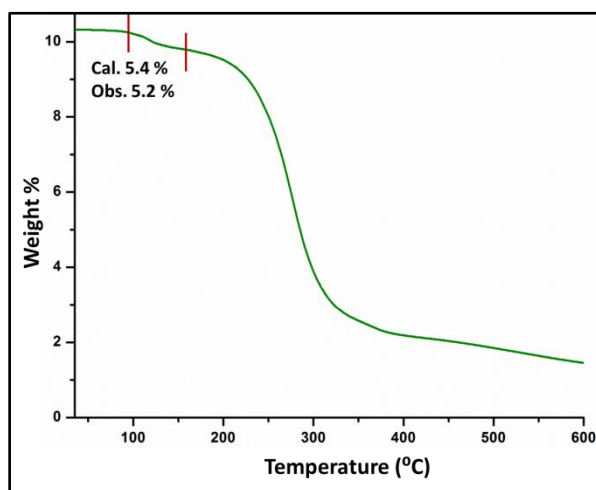
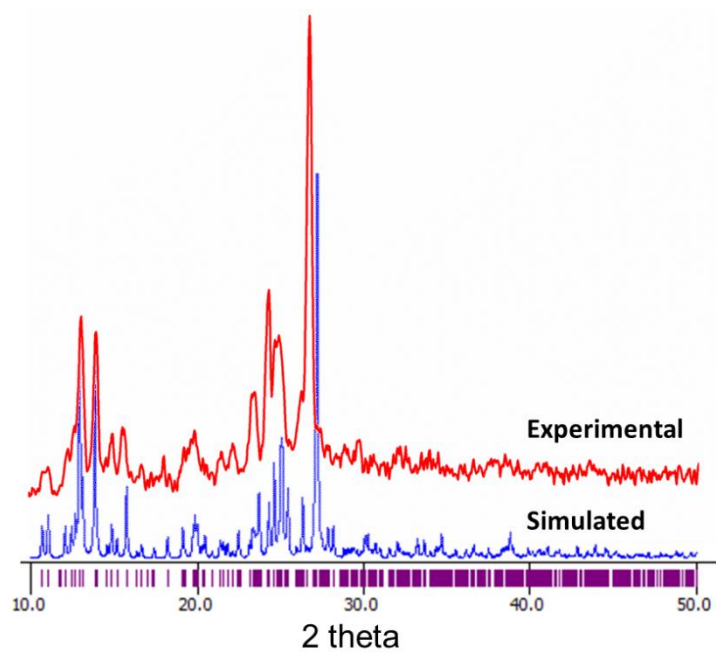
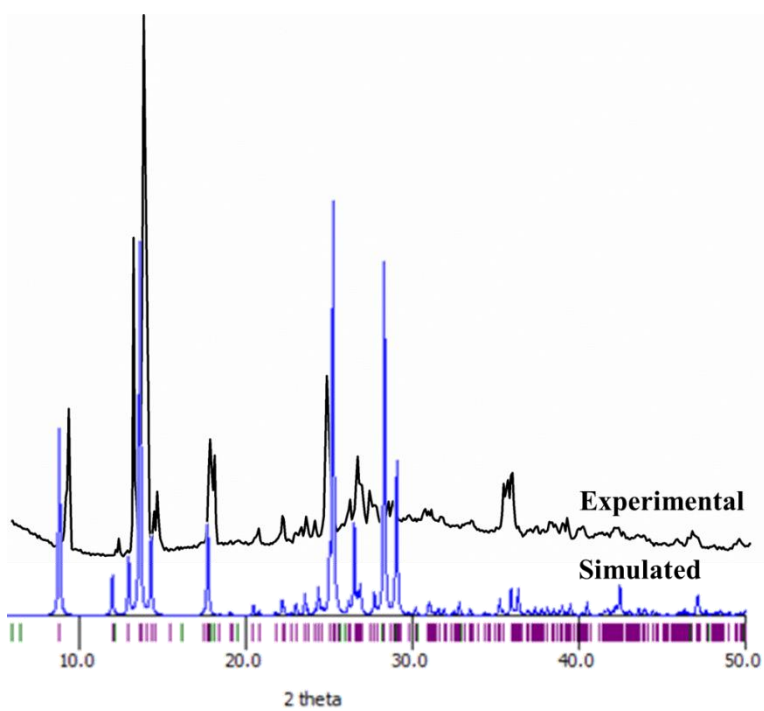


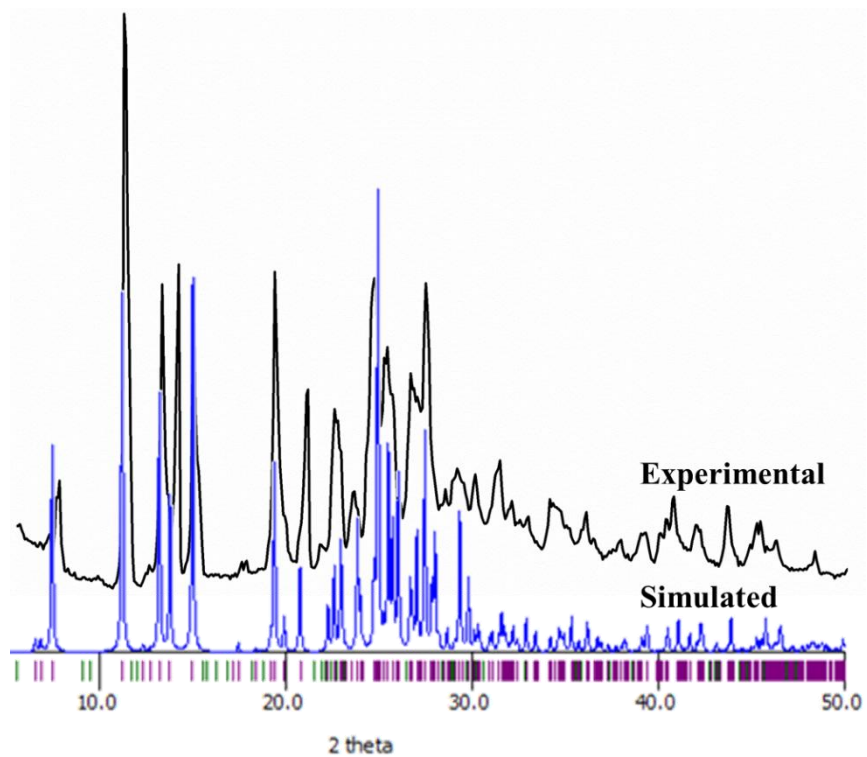
Fig. S3 Experimental PXRD pattern laid over simulated pattern from single crystal structure (**1** to **4**).



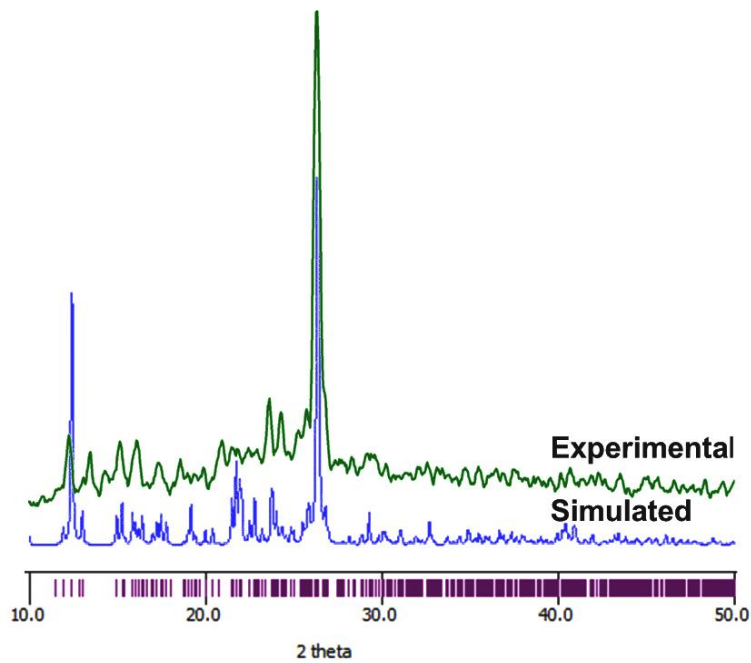
Cocrystal 1



Cocrystal 2



Cocystal 3



Cocystal 4

Table S3. Hydrogen bond parameters for cocrystals **1** to **4**

Cocrystal	Interaction	H...A/Å	D...A/Å	∠D-H...A/ Å	Symmetry code
1	O ₁₁ -H _{2A} ...O ₇	1.46	2.505(13)	164	1-x,1-y,1-z
	N ₁ -H _{5A} ...O ₁₉	2.19	3.013(16)	156	1-x,1-y,-z
	N ₂ -H _{6A} ...O ₁₀	2.04	2.940(15)	167	1-x,1-y,1-z
	O ₆ -H _{8A} ...O ₉	1.80	2.753(14)	168	1+x,1+y,z
	O ₁₂ -H _{9A} ...O ₁	1.73	2.640(13)	172	1-x,1-y,-z
	O ₂₀ -H _{20A} ...O ₁₂	1.87	2.749(14)	178	-1+x,y,z
	C ₂₁ -H ₂₁ ...O ₁₁	2.45	3.368(18)	168	-1+x,-1+y,z
	C ₂₂ -H ₂₂ ...O ₂₀	2.48	3.384(18)	164	x,-1+y,z
	C ₂₆ -H ₂₆ ...O ₅	2.36	3.242(17)	157	-1+x,-1+y,z
2	N ₁ -H _{1B} ...O ₁	1.97	2.853(16)	167	-
	O ₂ -H _{2A} ...O ₅	1.35	2.439(14)	165	-
	C ₁₆ -H _{16B} ...O ₃	2.59	3.531(19)	161	x,-1+y,z
3	O ₁ -H _{1A} ...O ₂	1.88	2.612(3)	164	-x,-y,-z
	N ₂ -H _{2B} ...O ₃	2.13	2.971(4)	174	1-x,-y,-z
	O ₃ -H _{3A} ...O ₄	2.16	2.922(3)	142	1-x,1-y,-z
	O ₄ -H _{4A} ...O ₅	1.70	2.629(3)	152	x,1+y,z
4	N ₁ -H _{1A} ...O ₁₀	2.02	3.035(7)	169	1-x,1-y,-z
	O ₁ -H _{2A} ...O ₂	1.47	2.659(6)	168	-x,-y,-z
	O ₃ -H _{3A} ...O ₁₅	1.93	2.775(7)	167	1-x,1-y,1-z
	O ₄ -H _{4A} ...O ₁₁	1.97	2.822(6)	165	-
	O ₆ -H _{6A} ...O ₁₀	1.85	2.692(6)	160	-1+x,-1+y,1+z
	O ₇ -H _{7A} ...O ₅	1.88	2.709(6)	160	1-x,-y,2-z
	O ₈ -H _{8A} ...O ₃	1.81	2.764(7)	171	-
	O ₉ -H _{9A} ...O ₁₂	1.78	2.650(6)	168	1-x,1-y,-z
	O ₁₁ -H _{11A} ...O ₁₆	1.84	2.743(8)	171	1-x,1-y,1-z
	O ₁₄ -H _{14A} ...O ₇	1.74	2.691(7)	166	2-x,1-y,1-z
O ₁₆ -H _{16B} ...O ₁₅	2.00	2.831(9)	172	-	

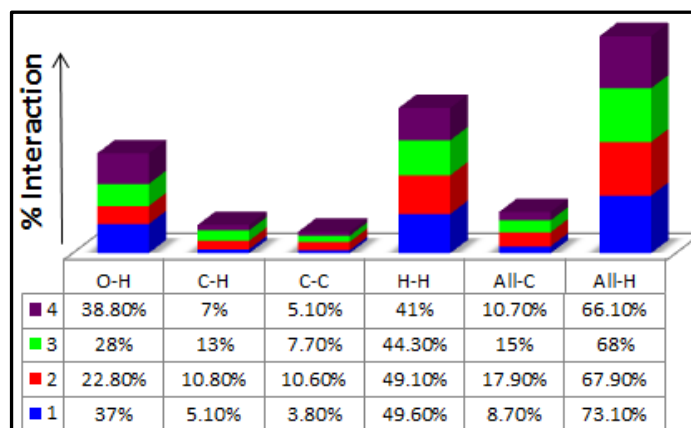
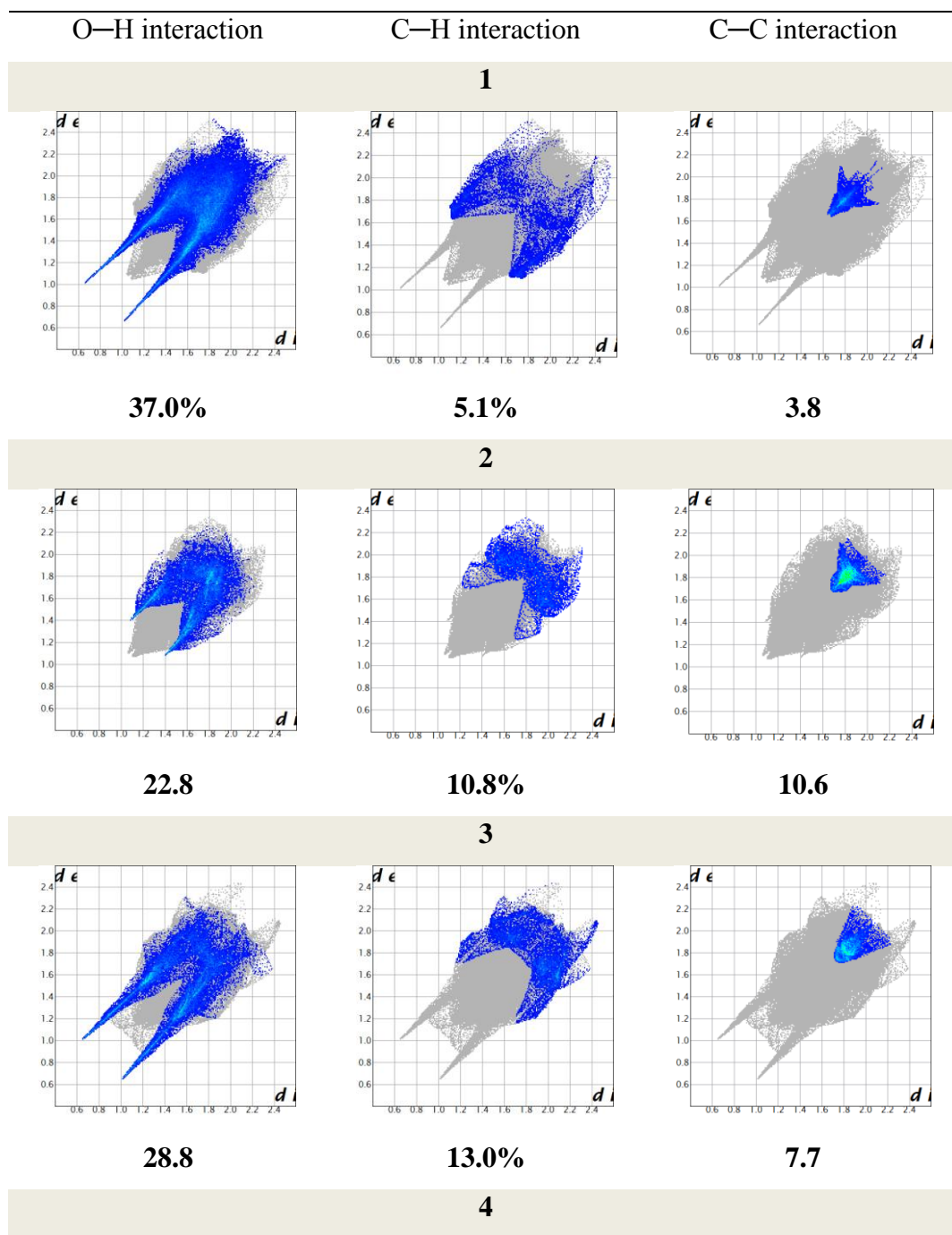
Fig. S4 Hirshfeld surface interaction in cocrystals **1** to **4**.

Fig. S5 Hirshfeld 2D finger print plots of the interactions in cocrystals **1** to **4**.



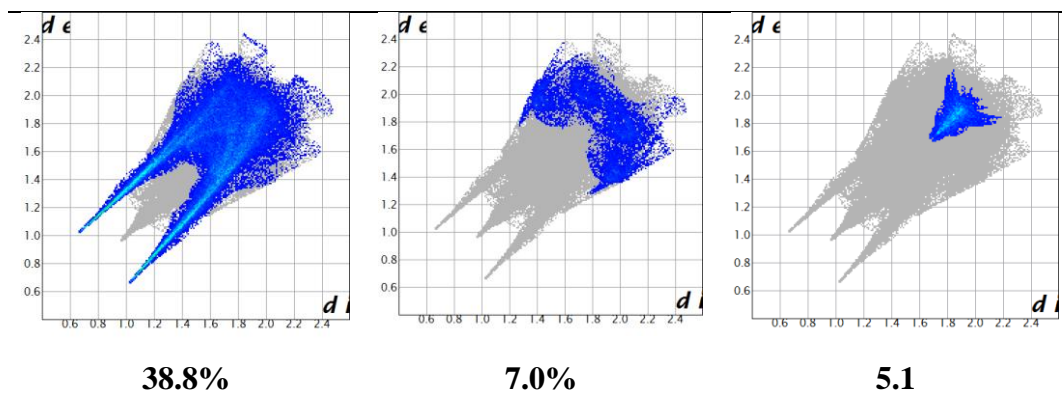


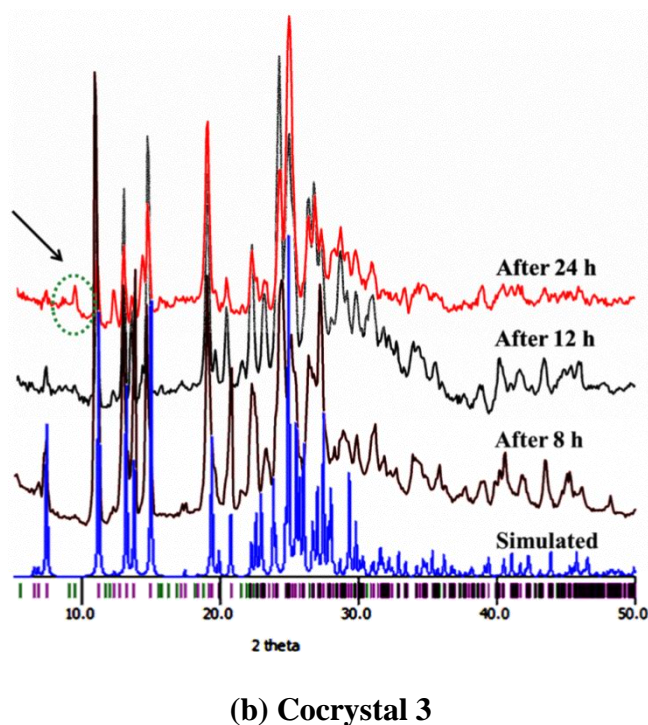
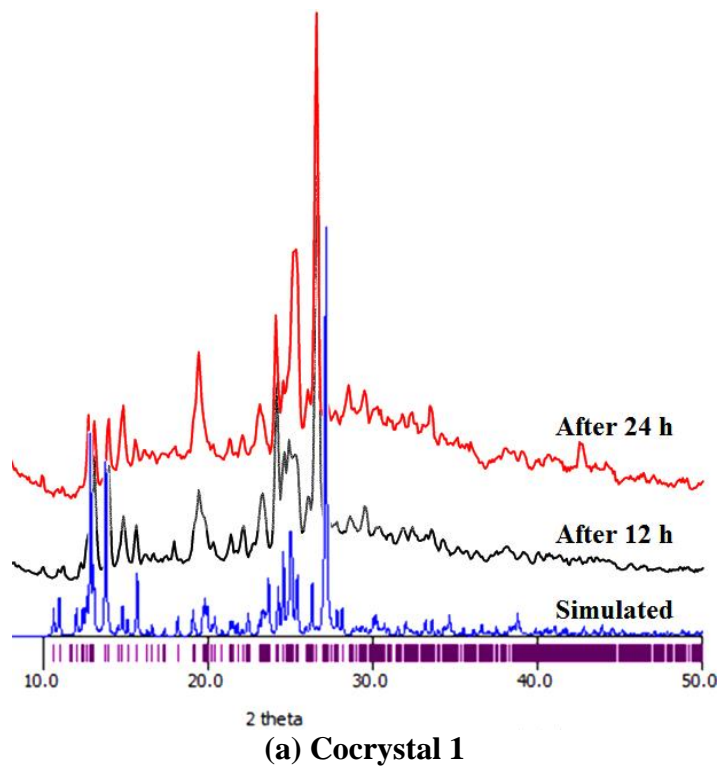
Table S4 Cambridge Structural Database (CSD) analysis for various synthons

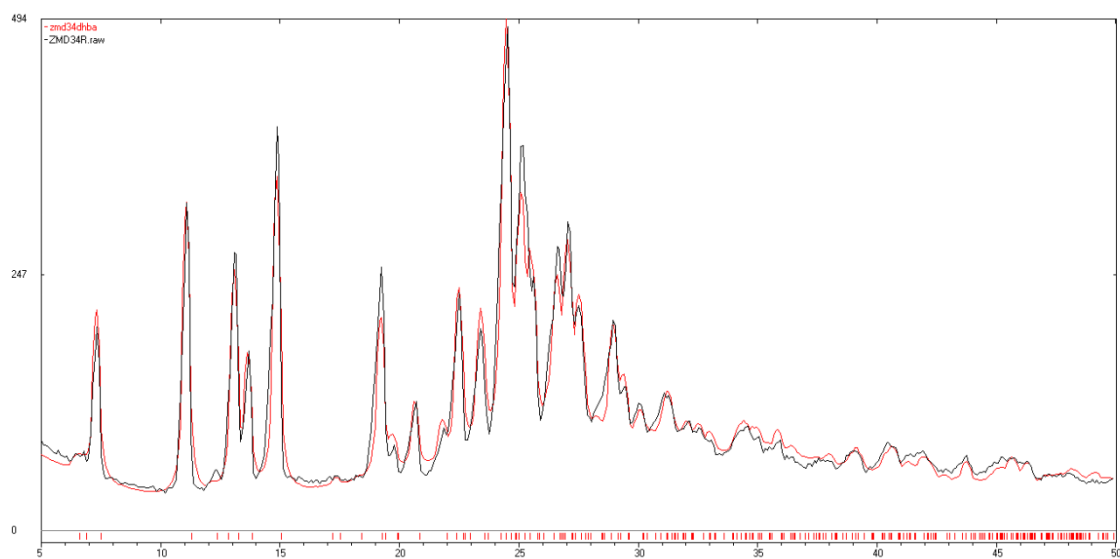
Search Limits: Structures with R factor less than 10%, no ions, no disordered and polymeric structures.

SYNTHON	REFCODE
<p style="text-align: center;">Synthon I</p>	FURWOG, FURXIB, ULAWAF04, ULAWAF06, ABULIU, ACEROR, ACERUX, ACONIR, AJAKEB, ASAXOH, ASAXUN01, BICQAH, BOBRAN, BUDWEC, CACGUK, EBONUG, ERIWUY, EXAQIE, EXAQOK, ERIWUY, JILZOU, JOWZIG, JOWZIG01, KINTUY, KOVSAR, KOVSEV, LATTOR, LATBOZ, LATTOR01, LOFLID, LUNMAI, LUNMEM, LUNMUC, LUNNAJ, LATBOZ, LUNNUD01, LUNPEP, LUNNIR, LUNNOX, LUNNUD, MOXVIF01, MUDVUE, NUHYEU, NUKXUN01, NUKXUN02, NUKYOI, NUKZOJ, OCEBUV, PAMWUX, PEQBES, PIRNOV, PIRNOV01, PIRPEN, PIRPIR, PIRQEO, PIRQIS, PIRREP, PEFGEO01, REBXED, REBXIH, REBXON, ROLFUU, RONDEE, ULAWAF, ULAWAJ, ULAWOT, ULAWUZ, ULAXAG, UMUYUX, UMUZAE, UYOSUX, UYOTAE, UYOTEI, UYOTOS, UYOVAG, VEJXAJ02, XICRAE, XOGMUD, XOXHEY, XOZSOV, YAGGOE, ZOHXAX
<p style="text-align: center;">Synthon II</p>	FOQRIO, LATBOZ, REBXED, REBXIH, XOXHEY, MOXVIF, MOXVIF01, MOXVOL, MOXXAZ, NUHYEU, PEFGEO01, PEFGEO02, ZOYCEX, ZOHXAX, ZOYCOH
	FURXUN, ACESOS, AJAKIF, AJAKUR, AJALEC, BIZTIP, BOBQUG, BUDZUV, BUFQAU, CUYXUQ, DAVPAS, DAVPEW, DINRUP01, EVETAB, EBOSIX01, ESATUN, ERIWUY, FOTFIF, FOTFOL, FOTFUR, FURAOX, GENLIV, GENLOB, GEQXIL, GESBAJ, GESBEN, GESBUD, GESCIS, GESCUE, GOGYUX, HIBGOP, HIQSEH, HIQMAX, HIQRIK, HIQSIL, HIQROQ,

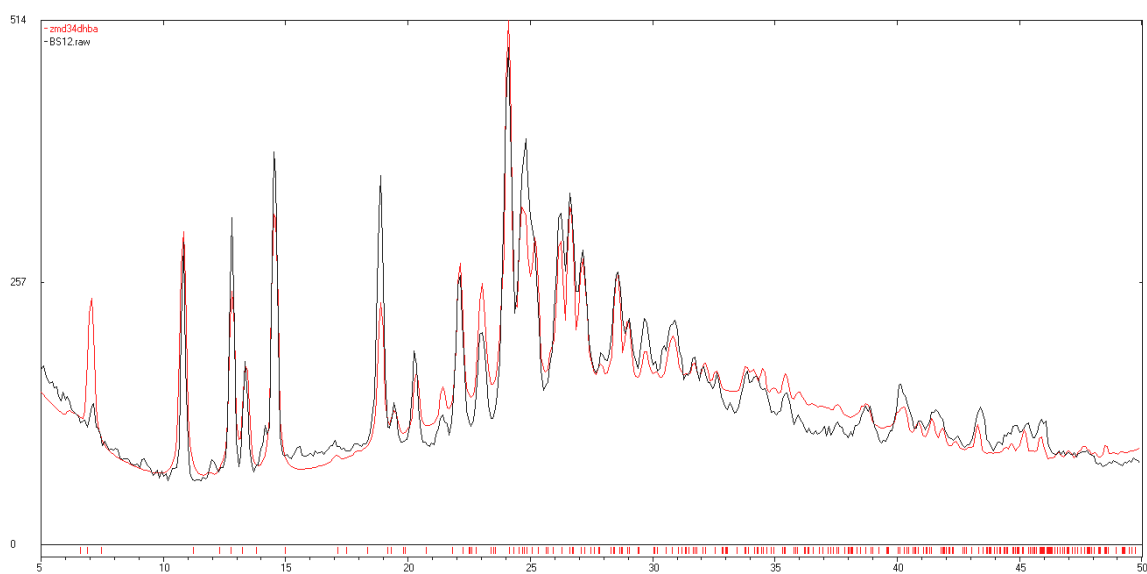
8	REHSOO	172, 176
9	REHSUU	178
10	REHTAB	175
11	VAKTOS	176
12	VAKTOS01	173
13	VUHFIO	175
14	VUHFIO01	179
15	WUZHOP	178
16	WUZHOP	165
17	WUZJEH	172
18	WUZKIM	175
19	ZIMBEE (HCL salt of ZMD)	177
20	ZIMBII (HBr salt of ZMD)	179
21	ZIMCAB (Perchlorate salt of ZMD)	173
This Work		
	Cocrystal	Dihedral angle
	1	172, 171
	2	176
	3	179
	4	165

Fig. S6 Stack plots of PXRD pattern of slurry experiment of **1** (a) and **3** (b) attributing phase stability of materials in aqueous medium. Transformation of cocrystal **3** into possible hydrate formation monitored at 8h (c), 12h (d) and 24h (e) intervals.

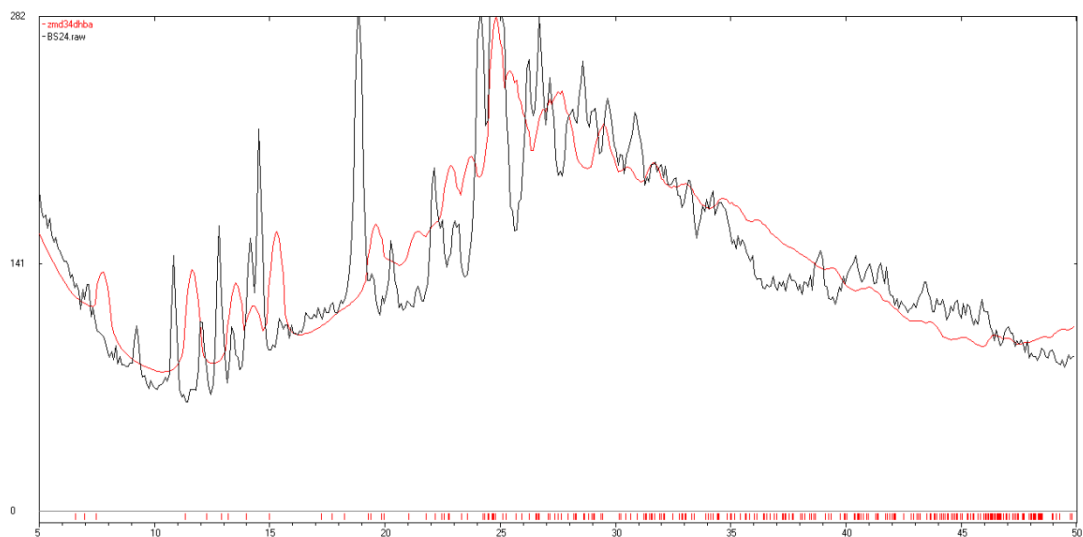




(c) Rietveld refinement for the slurry of cocystal **3** after 8h indicates phase stability.

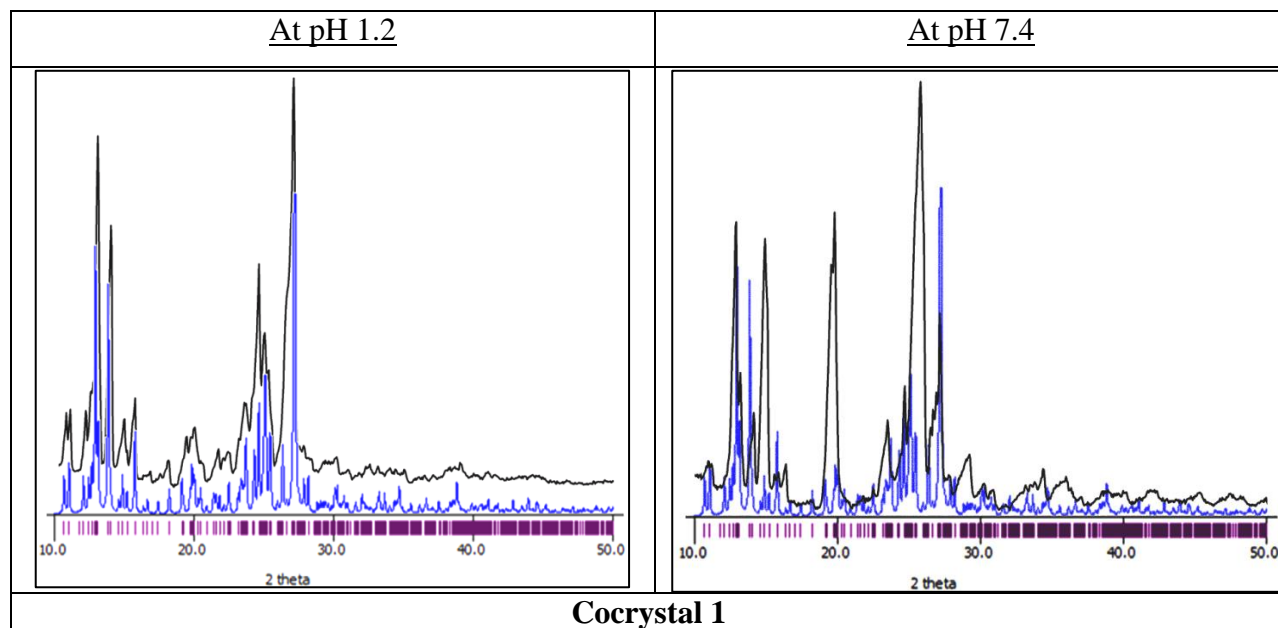


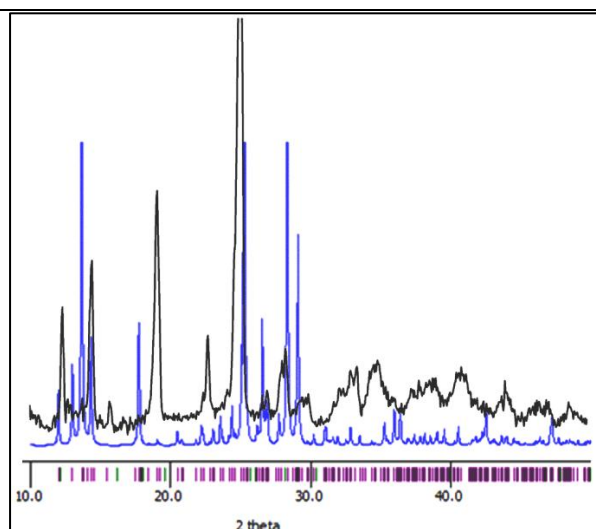
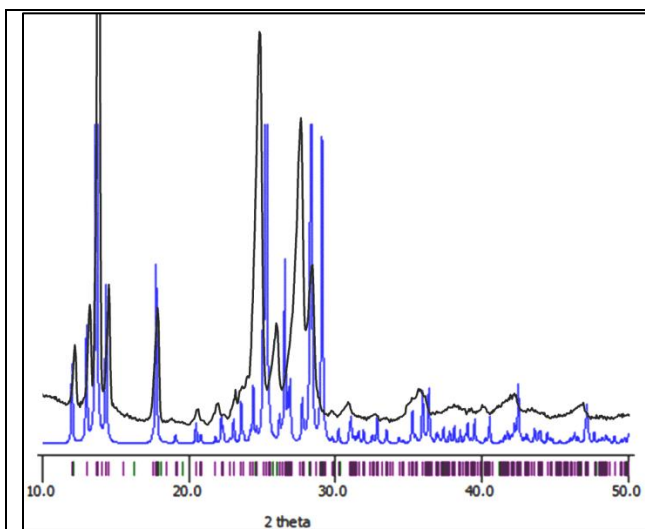
(d) Slurry of cocystal **3** shows phase stability even after 12h.



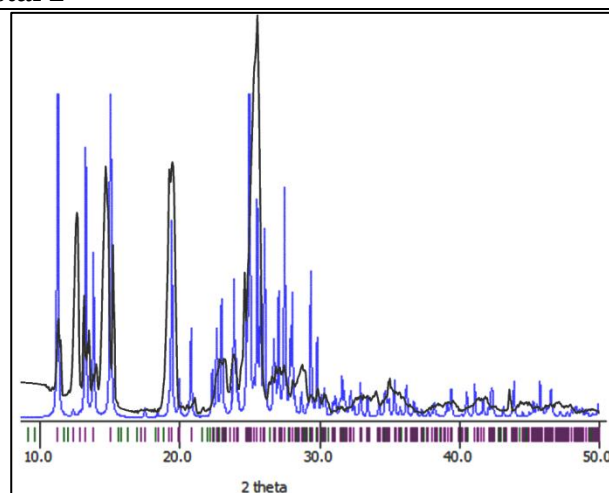
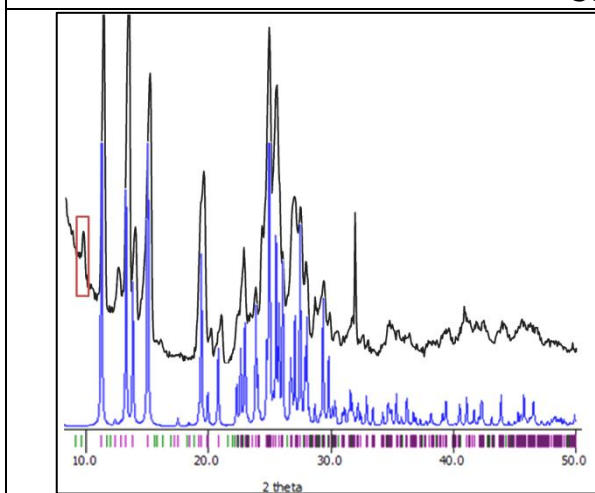
(e) Cocystal **3** has transformed after 24h into its possible hydrates formation

Fig. S7 Stack plots of PXRD pattern of simulated (blue) and slurry experiment (black) obtained after 12 h revealing the phase stability of cocystals (**1** to **4**); however **4** transforms to its anhydrous form.

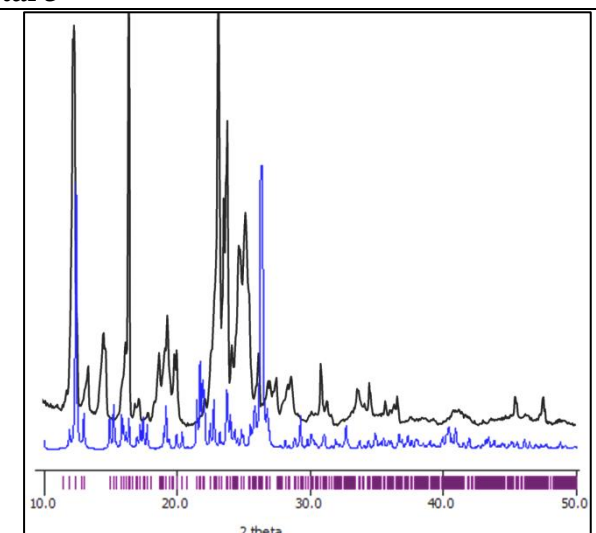
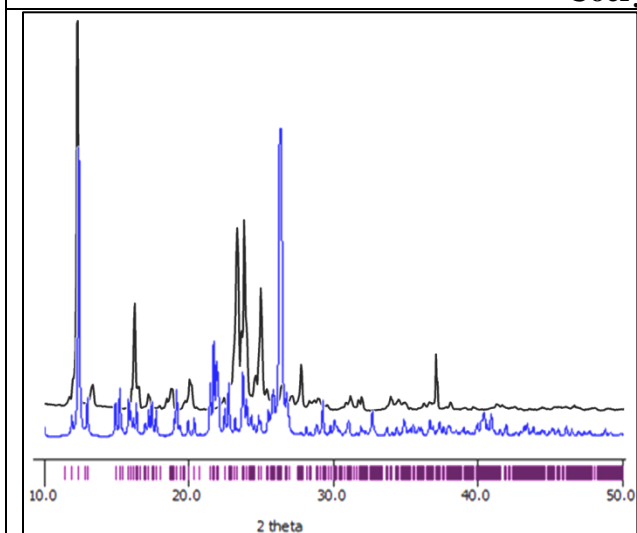




Cocrystal 2



Cocrystal 3



Cocrystal 4

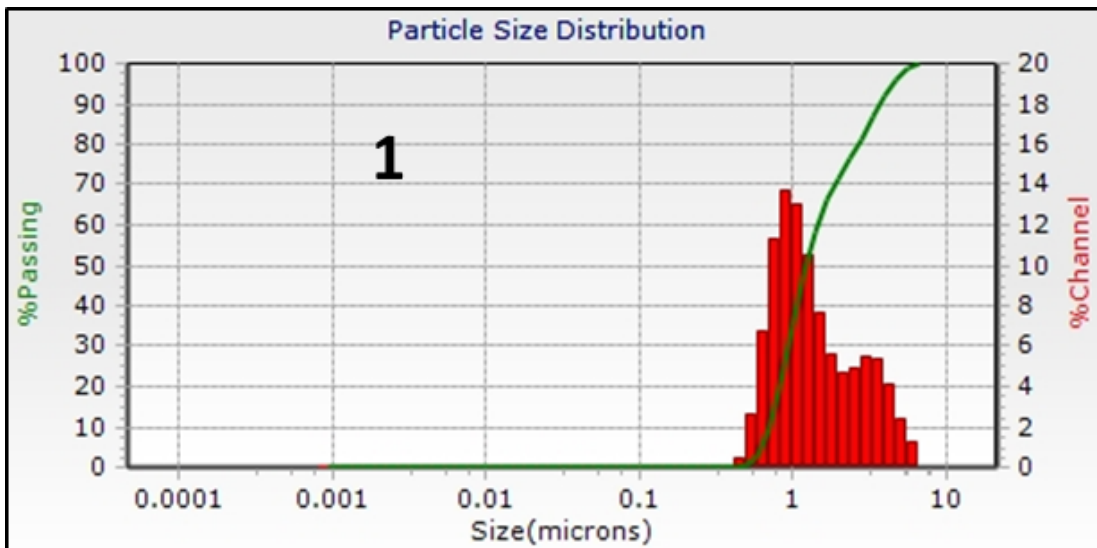
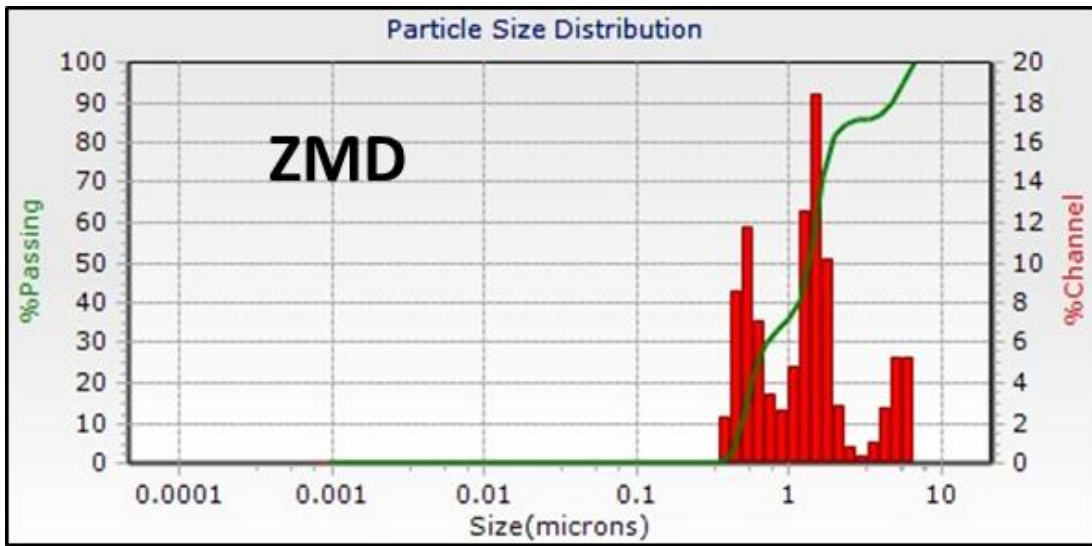
Solubility experiment

An excess amount of drug (ZMD) and its cocrystal (**1** to **4**) was added to 3 ml of the buffer at ambient temperature in a jacketed water vessel connected to a circulating water bath. The mixture was stirred at a rate of 80 rpm. We maintained the temperature of syringes, pipettes, filters, vials and needles utilized in experiments by preheating at same temperature in an oven. The solubilities observed after 12 h are an average of at least two determinations. Experiments were performed in Agilent Cary-60 double beam UV-vis Spectrophotometer. The solubility parameter was calculated using the formula $C_u = (A_u - \text{intercept}) / \text{Slope}$, where C_u and A_u being the concentration and absorbance of unknown solution. The solubilities quoted were further correlated with that obtained from gravimetric measurements. A third set of experiment was also performed for solubility determination in pure water. To understand the change in solubility behaviour particle size distributions (PSD) were determined using dynamic light scattering (DLS) method for at least three samples. Cocrystal **1** & **3** were subjected for PSD study intentionally in order to identify similar and improved solubility when compared with ZMD. Interestingly, the particle size distribution of **1** is nearly identical (~0.8-4.0 micron) with ZMD (~0.7-3.5 micron) thereby making not much difference in its solubility. However, the particle distribution for cocrystal **3** clearly indicated smaller particle size distributions (~0.001-0.005 micron) than ZMD. Nearly 10% particles are populated at higher size scale may be due to agglomeration of particles (Figures below).

Table S6 (a) Solubility of ZMD and its cocrystals (**1** to **4**) at different pH conditions

Drug	Solubility (mg/mL) at		
	Water	pH 1.2 buffer solution	pH 7.4 buffer solution
ZMD	0.034	0.533	0.030
1	0.036	0.008	0.003
2	0.053	0.184	0.266
3	0.085	0.132	0.142
4	0.037	0.186	0.376

(b) Particle Size Distribution plots for pure ZMD, cocrystal 1 & 3



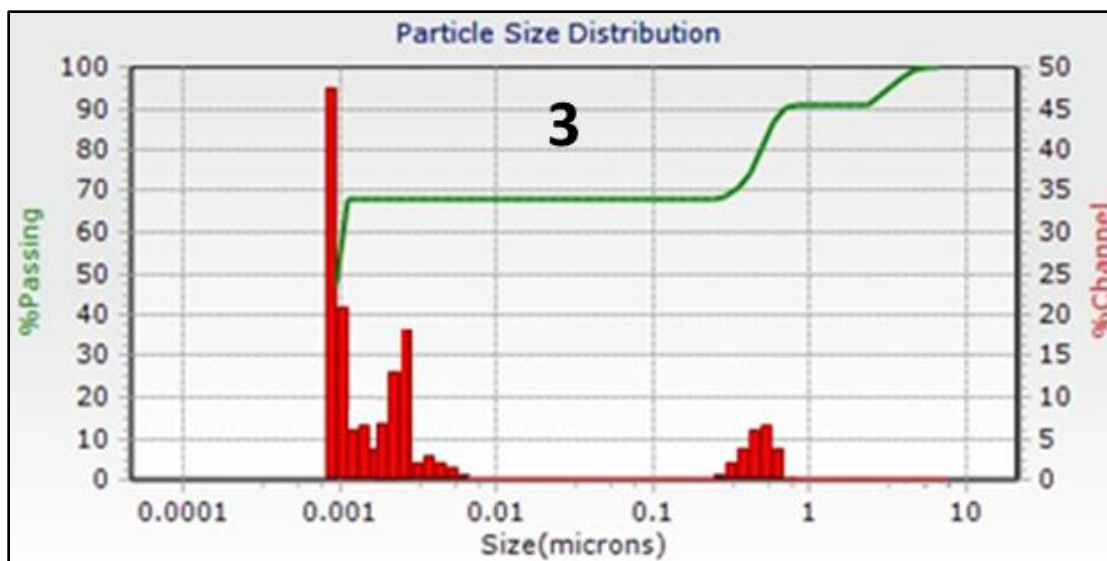
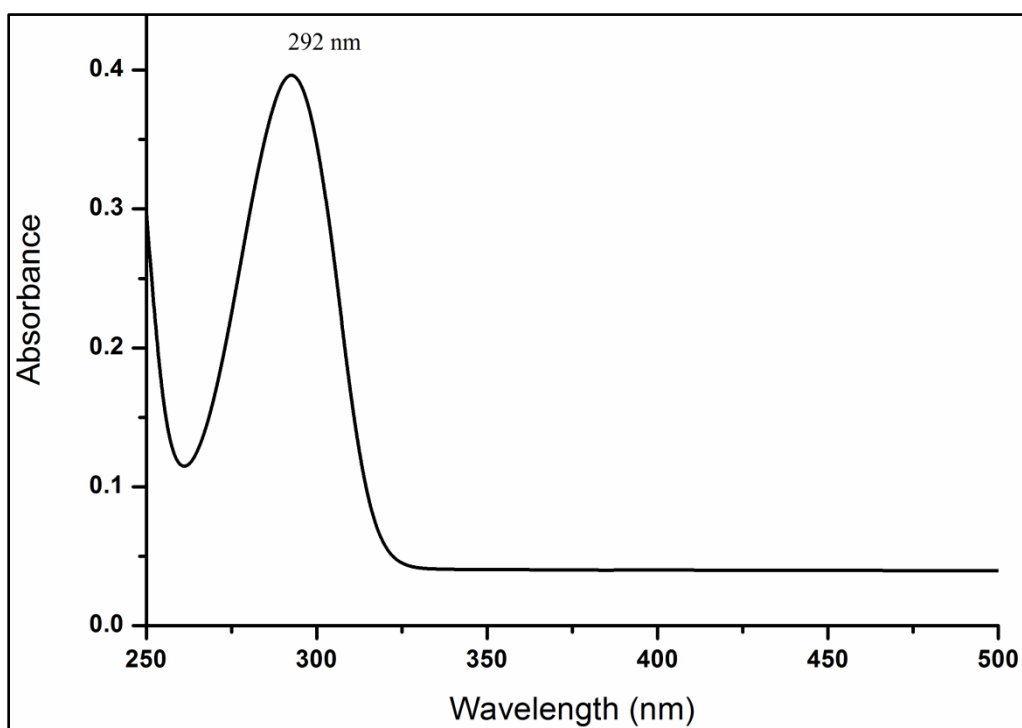
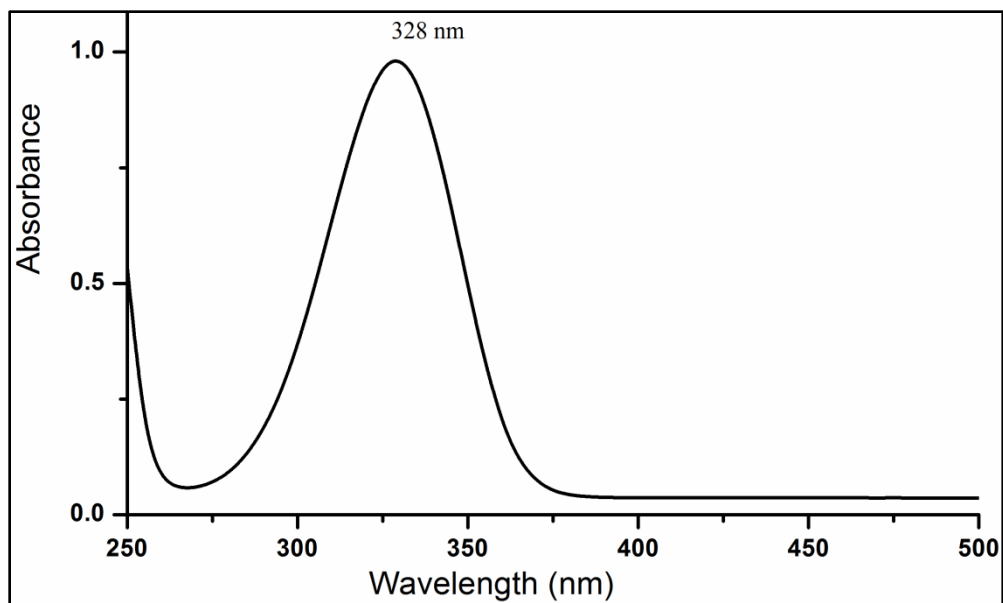


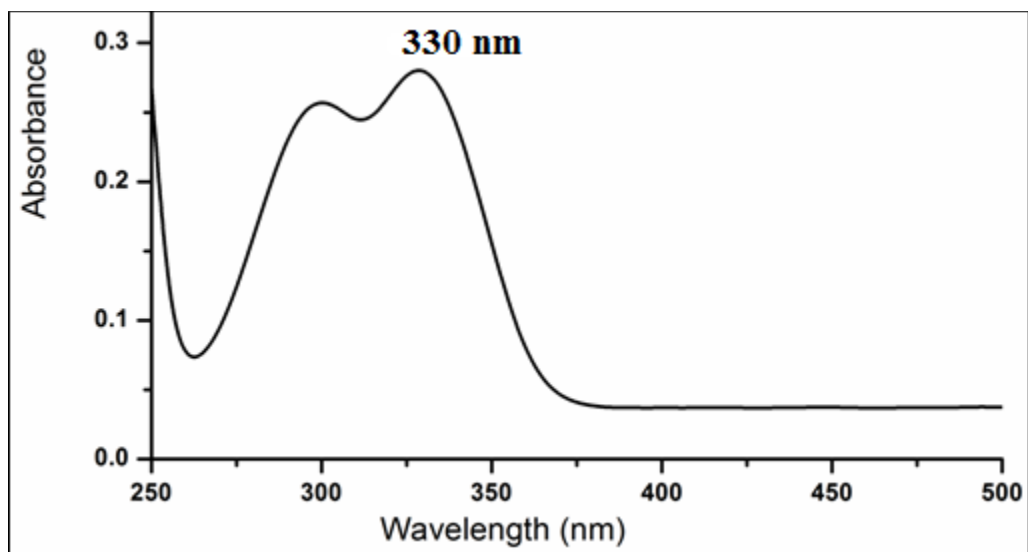
Fig. S8 UV spectra of ZMD and its cocrystals (1 to 4) at different pH conditions.



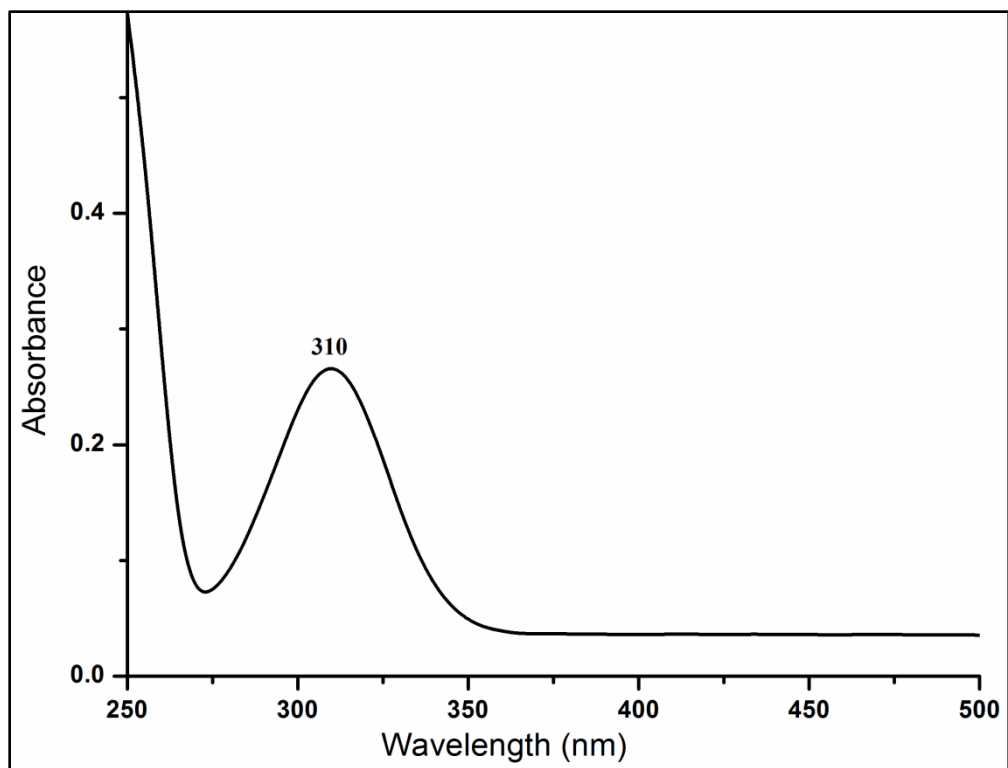
ZMD at pH 1.2



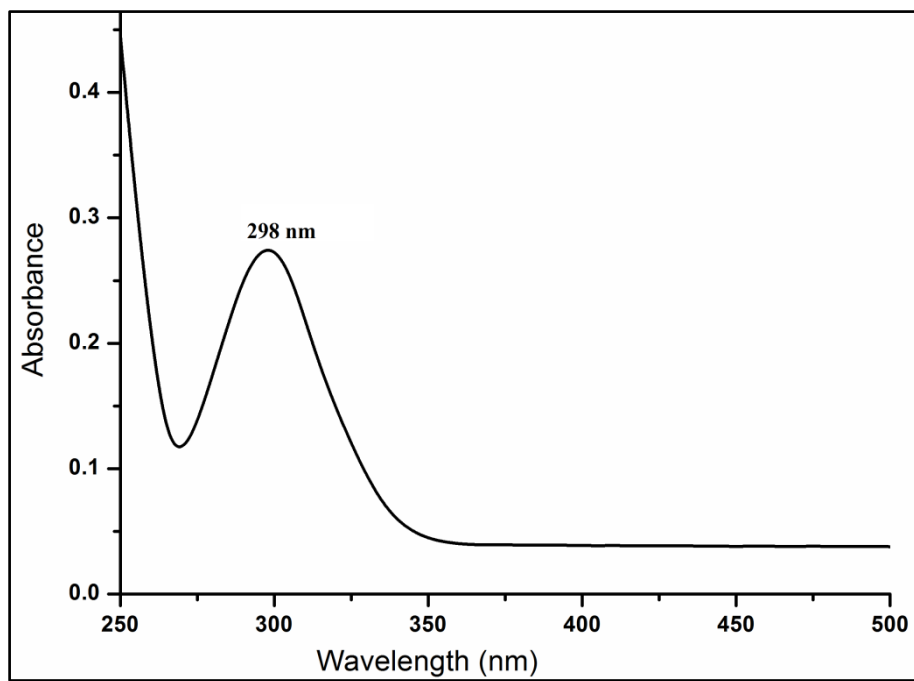
2,5-DHBA at pH 1.2



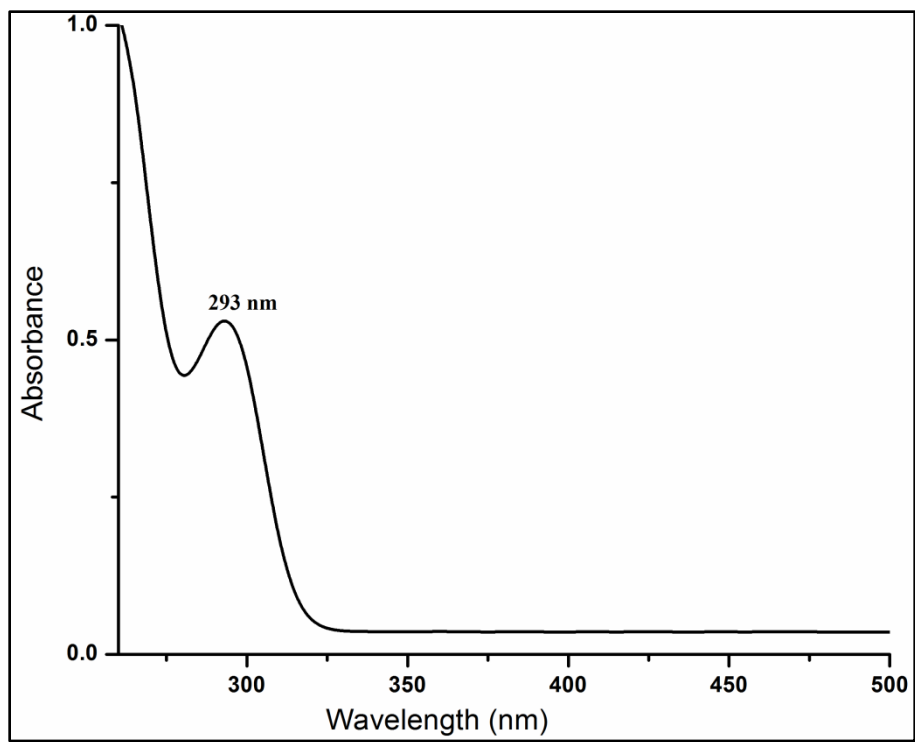
Cocrystal 1 at pH 1.2



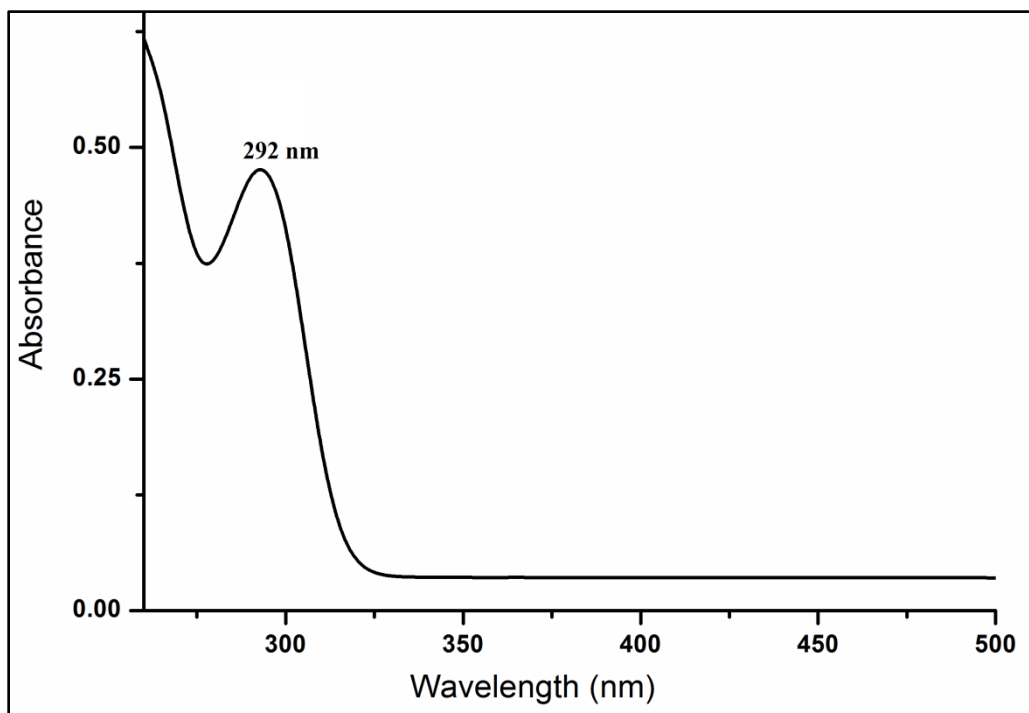
2,6-DHBA at pH 1.2



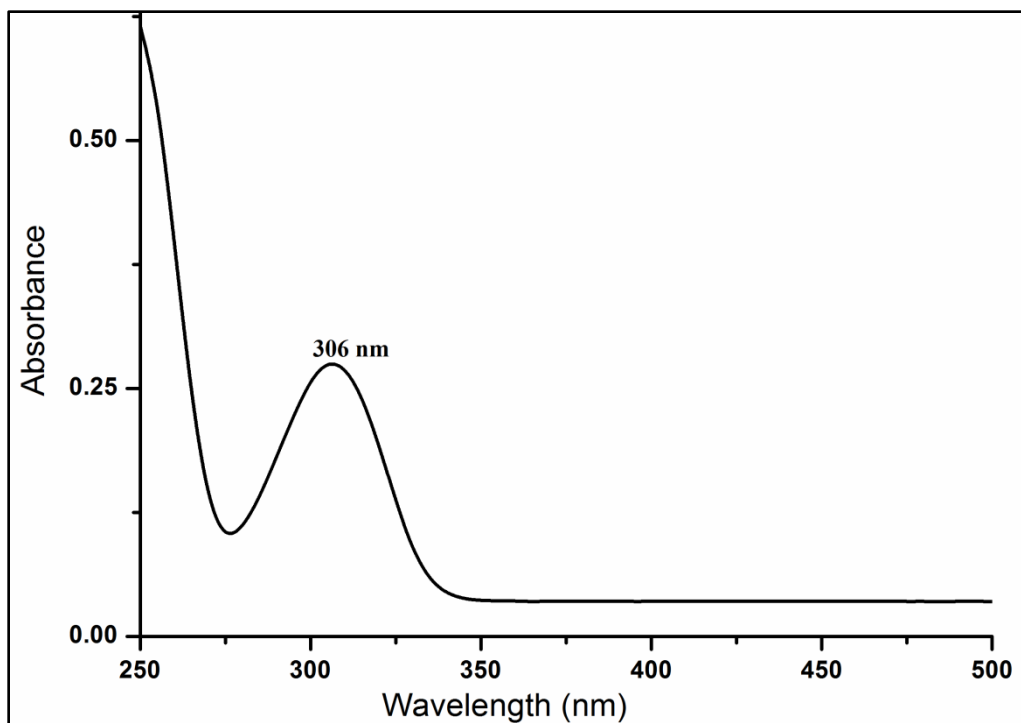
Cocrystal 2 at pH 1.2



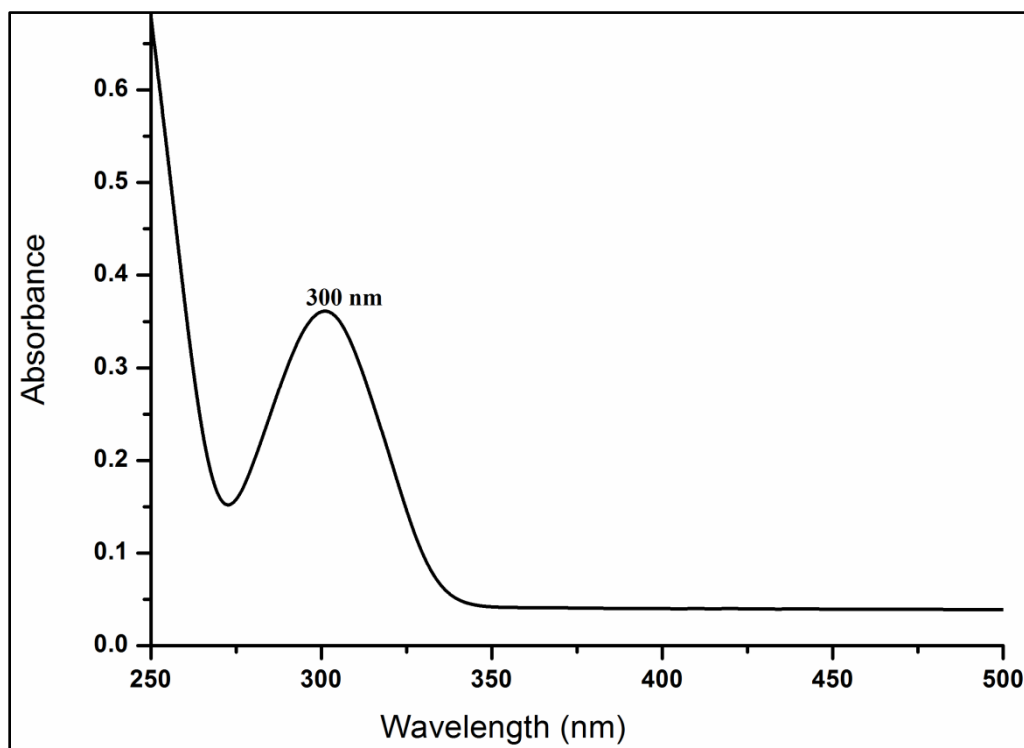
3,4-DHBA at pH 1.2



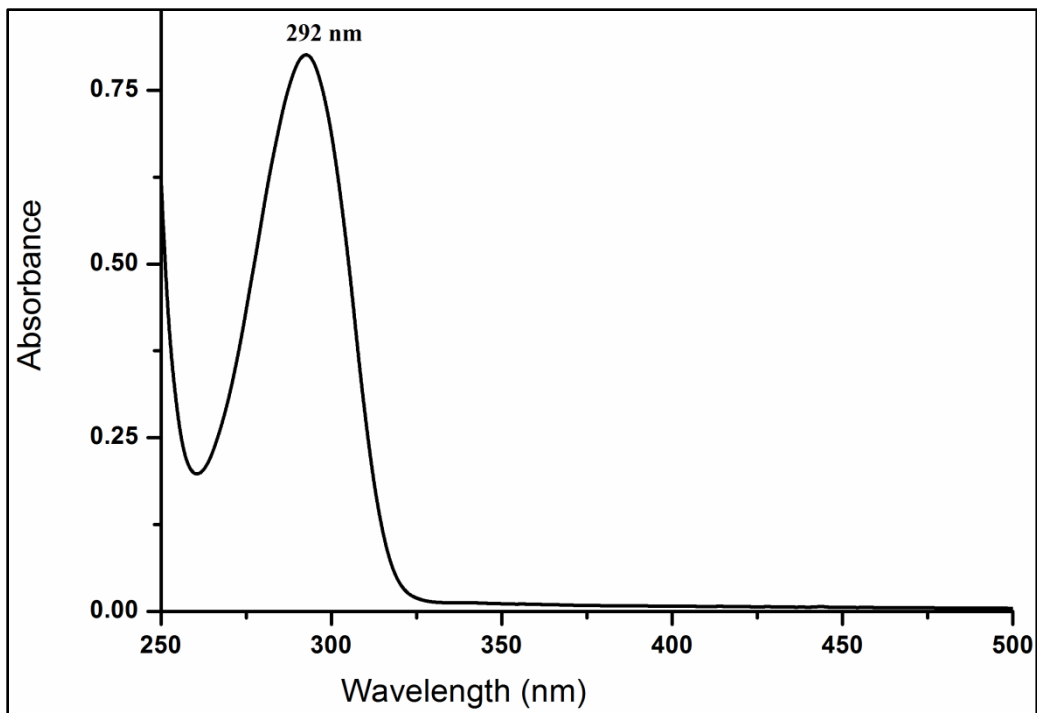
Cocrystal 3 at pH 1.2



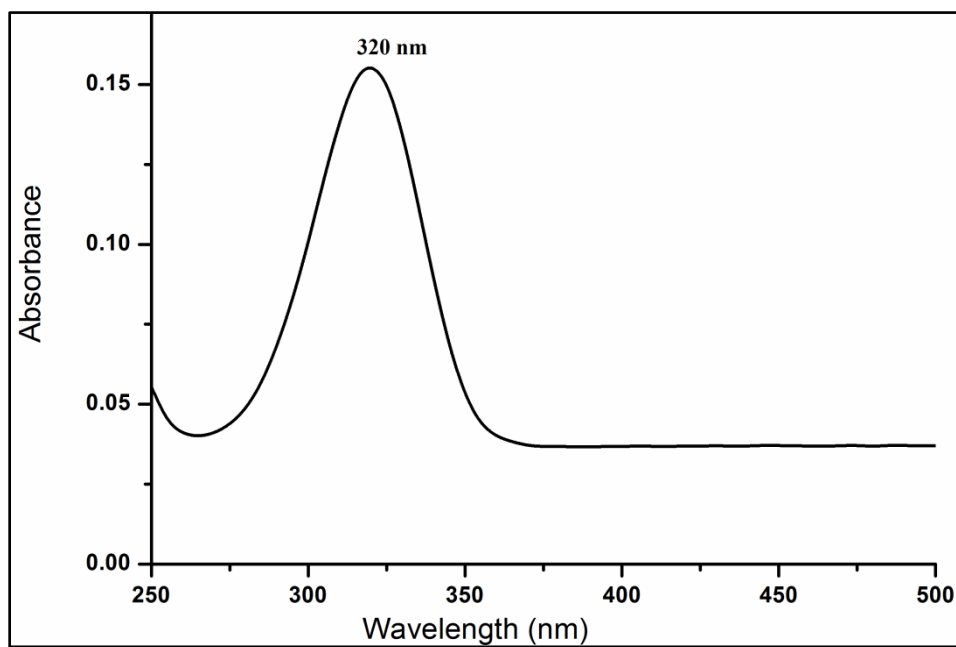
3,5-DHBA at pH 1.2



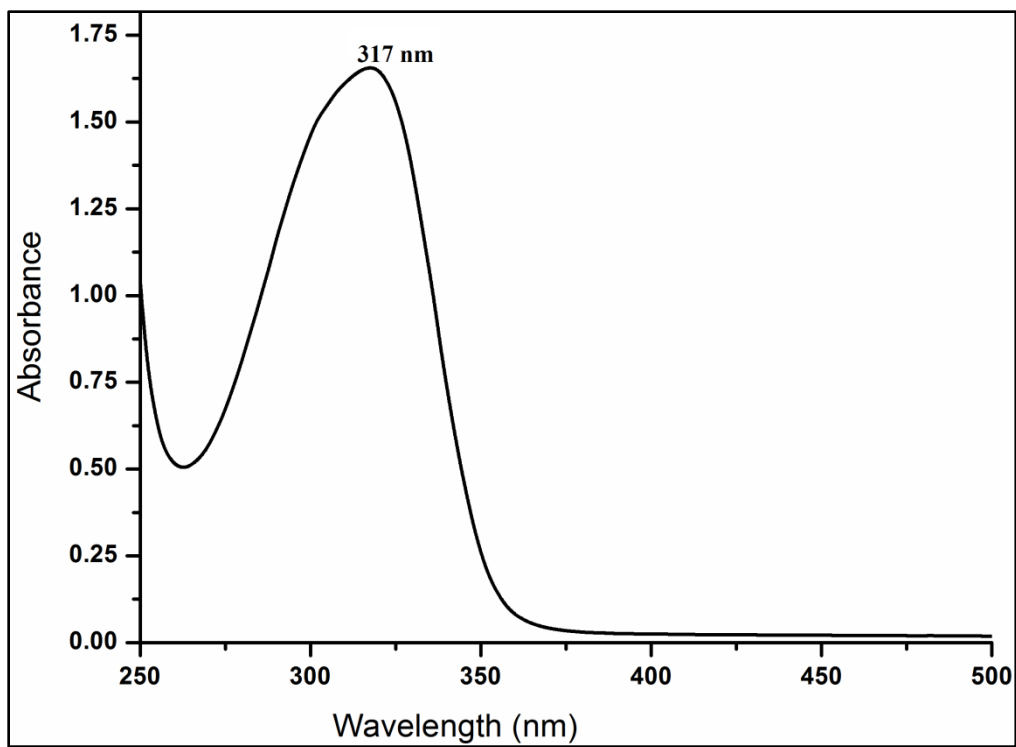
Cocrystal 4 at pH 1.2



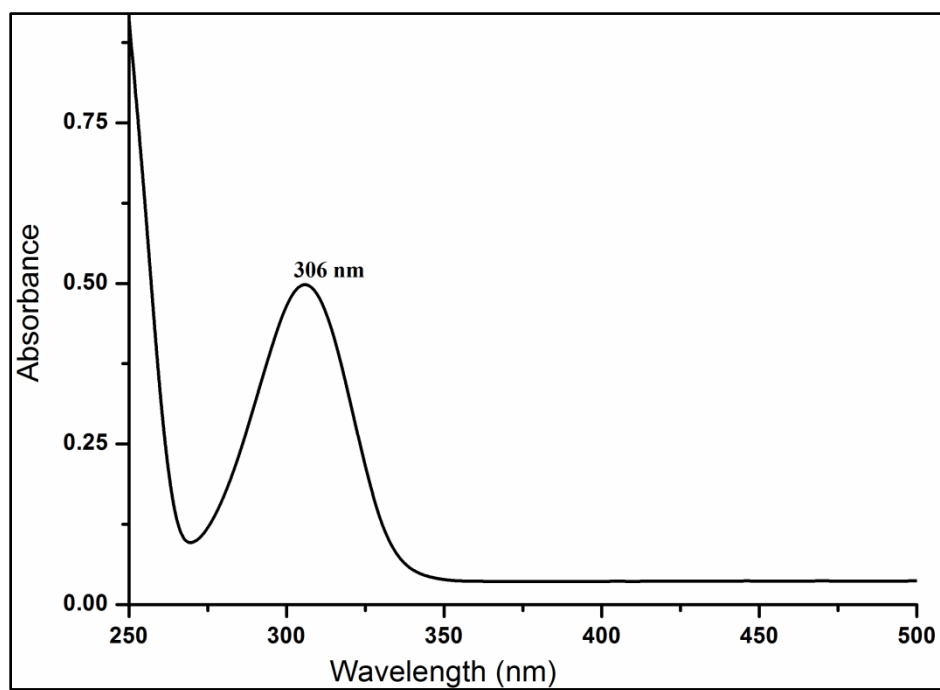
ZMD at pH 7.4



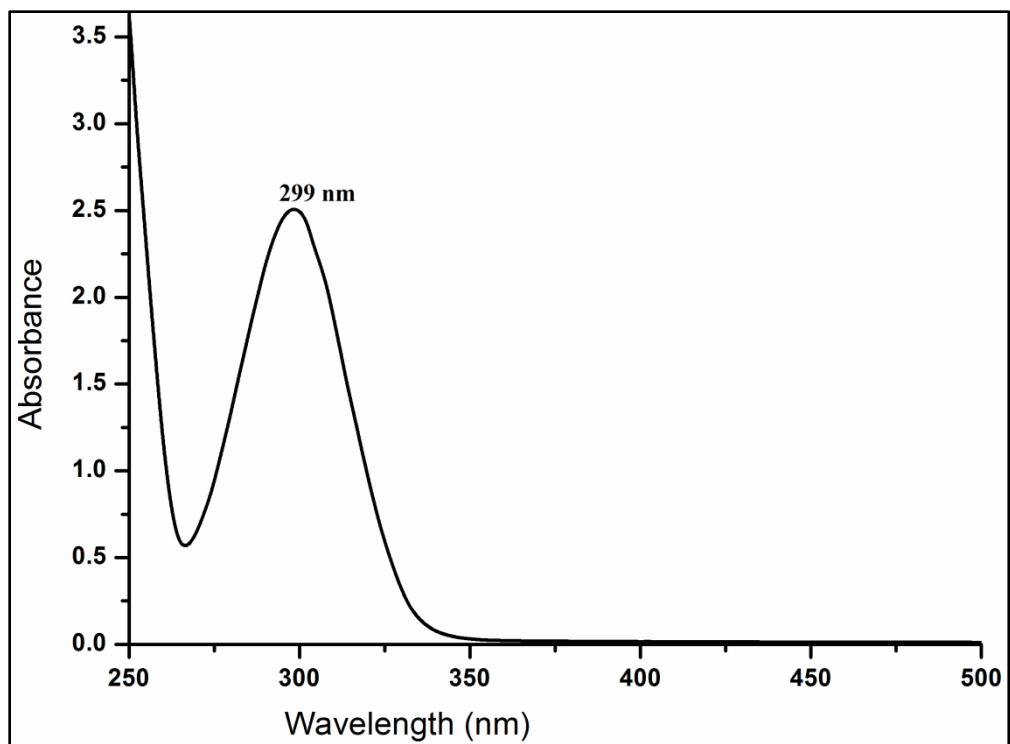
2,5-DHBA at pH 7.4



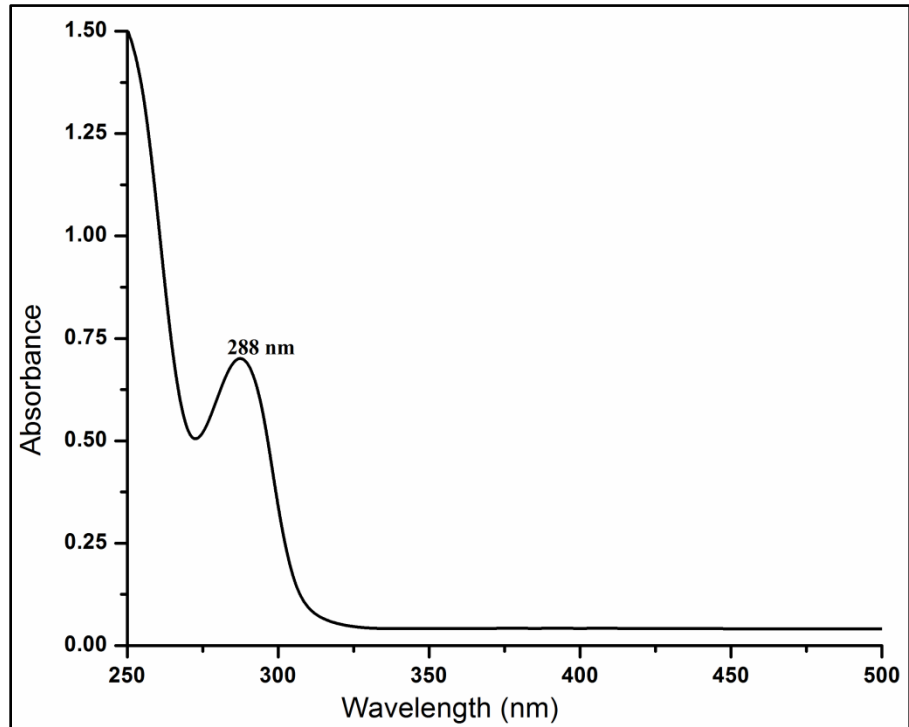
Cocystal 1 at pH 7.4



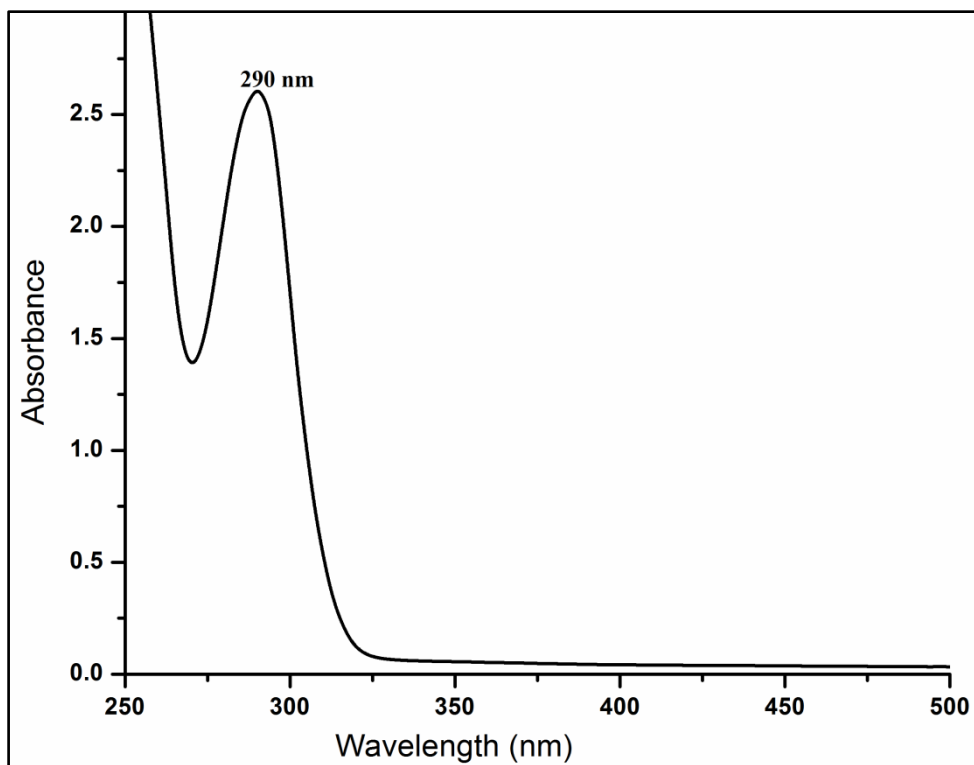
2,6-DHBA at pH 7.4



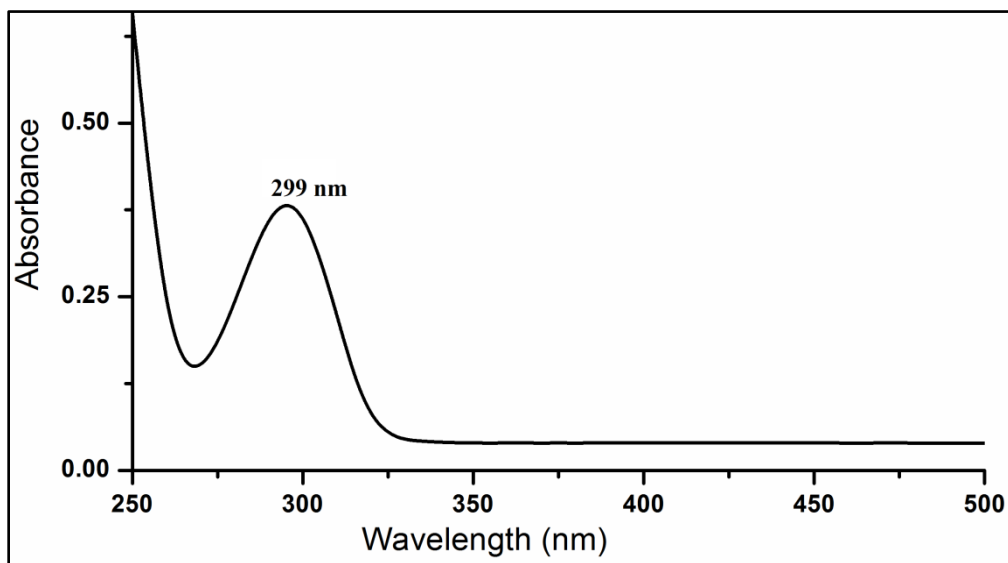
Cocystal 2 at pH 7.4



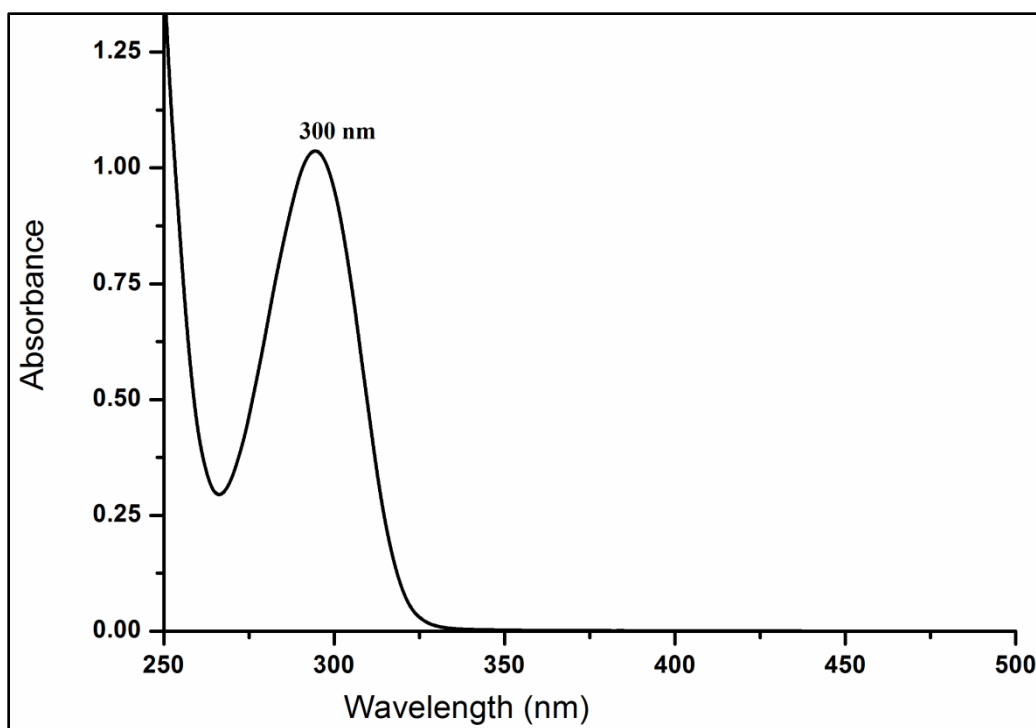
3,4-DHBA at pH 7.4



Cocystal 3 at pH 7.4



3,5-DHBA at pH 7.4

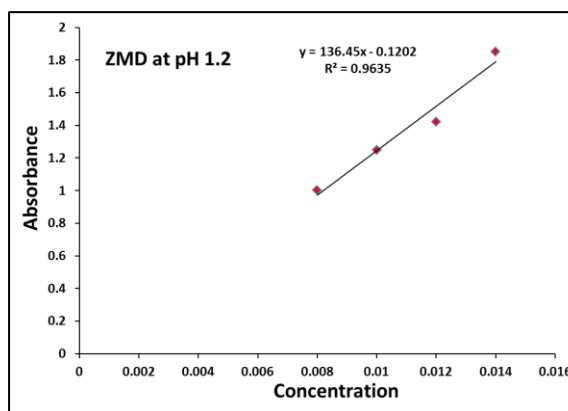
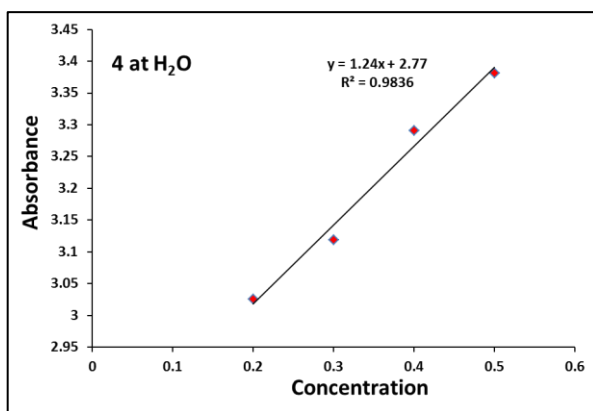
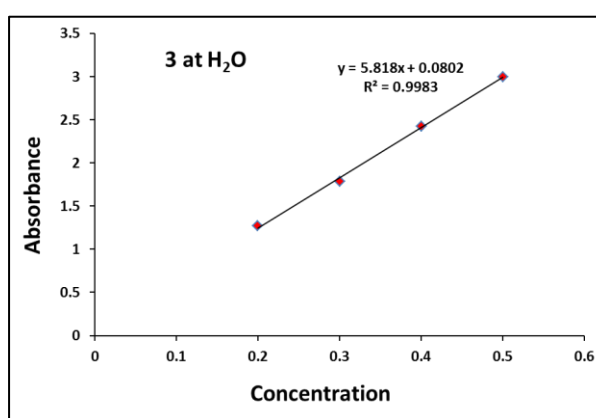
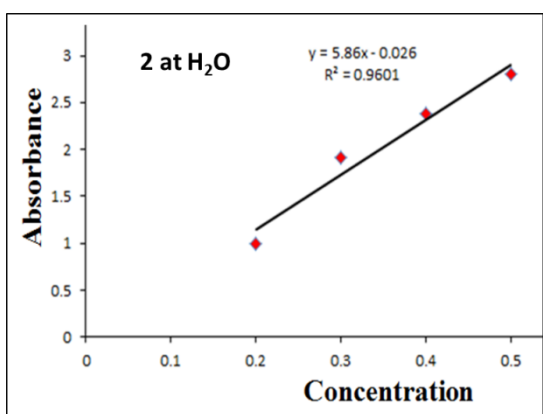
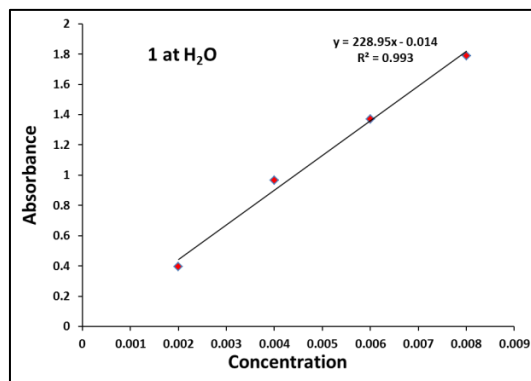
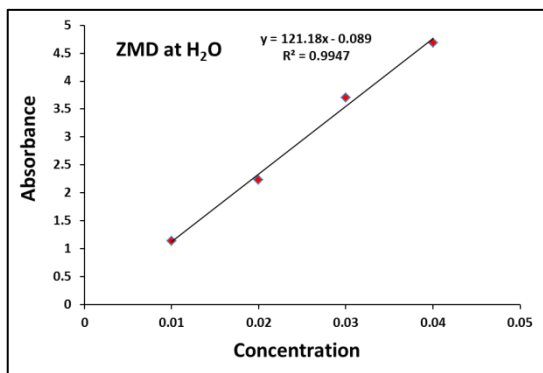


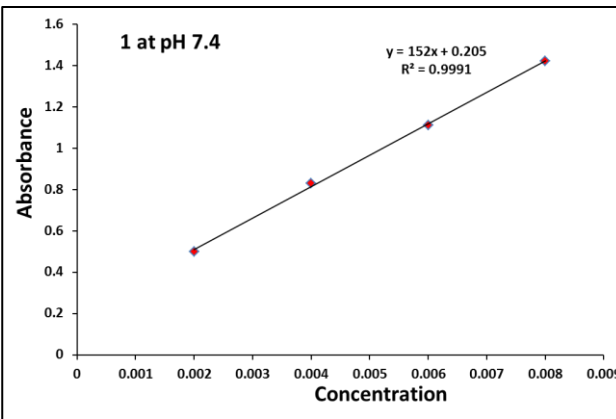
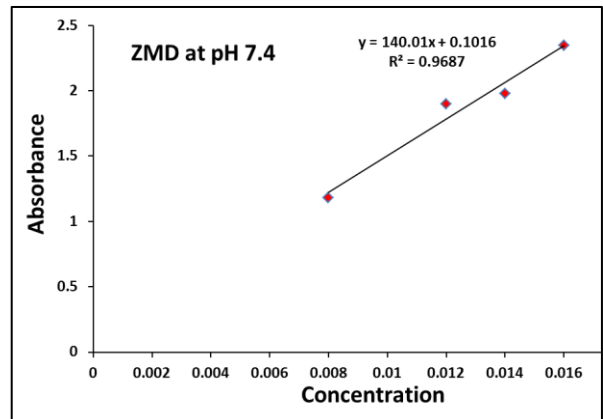
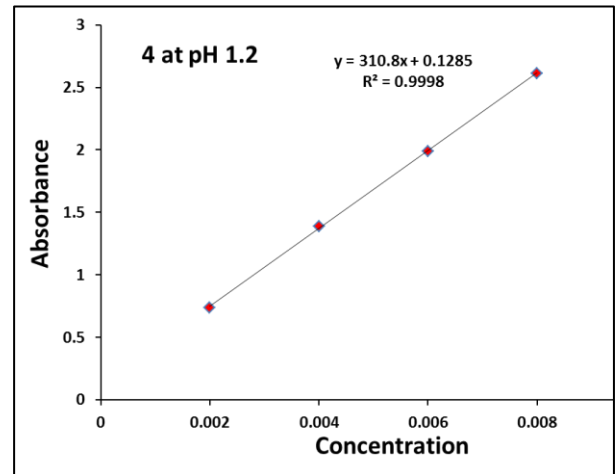
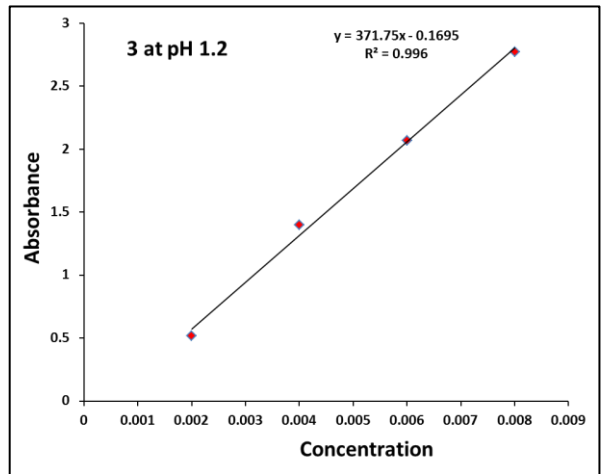
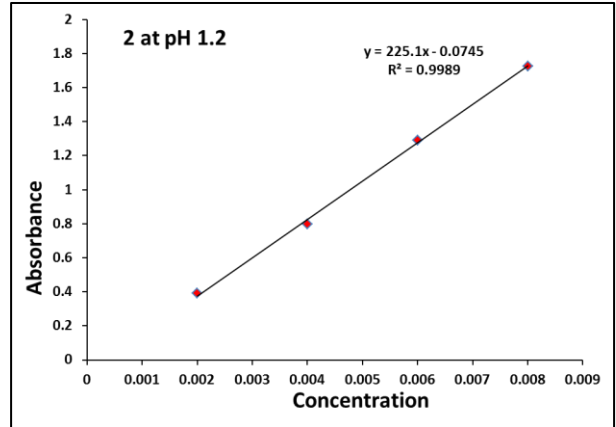
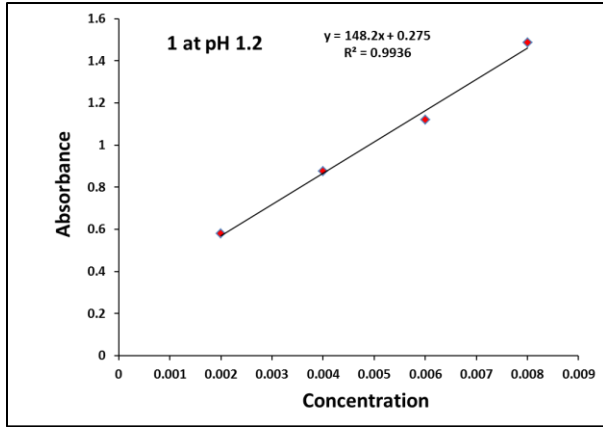
Cocystal 4 at pH 7.4

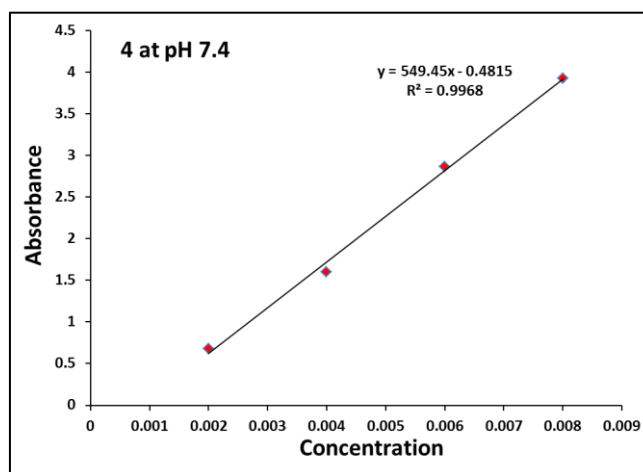
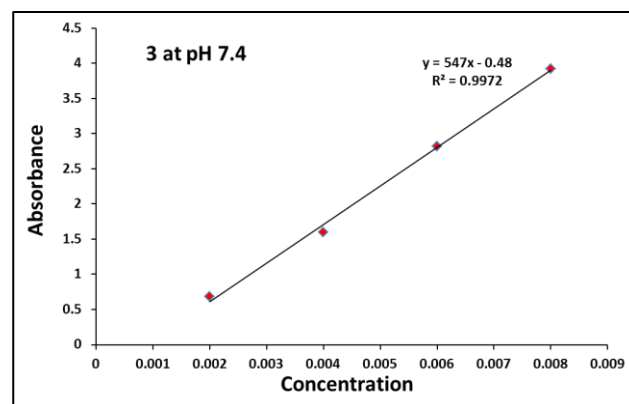
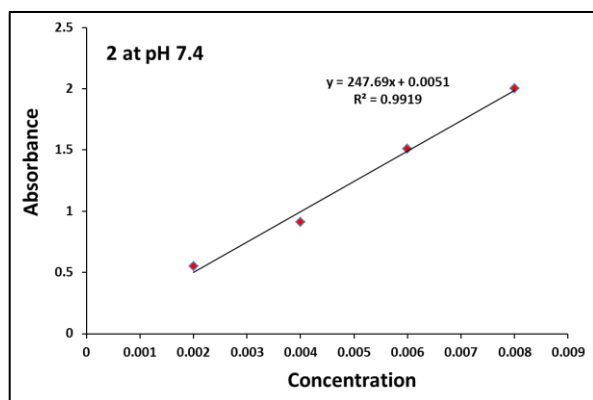
Table S7 Wavelength value corresponding to the absorbance considered in calculating solubility and permeability parameters.

Material	Wavelength (nm)	
	At pH 1.2	At pH 7.4
ZMD	292	292
2,5-DHBA	328	320
Cocystal 1	330	317
2,6-DHBA	310	306
Cocystal 2	298	299
3,4-DHBA	293	288
Cocystal 3	292	290
3,5-DHBA	306	299
Cocystal 4	300	300

Fig. S9 Calibration curves for solubility determination of ZMD and cocrystals **1** to **4**.







Diffusion/Permeation study

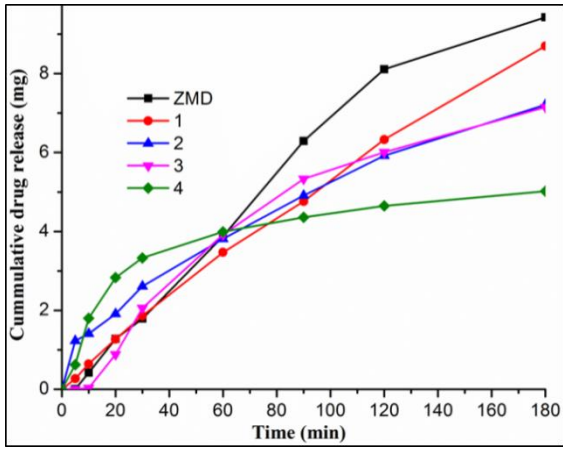
Diffusion/permeability experiment of the API and the synthesized four cocrystals was performed in a diffusion apparatus using cellulose membrane (MW 14000, Himedia, India) following the reported procedure by Desiraju et al. Diffusion behavior was studied at buffer solution with two different pH (i.e. 1.2 and 7.4). Prior to this experiment the membrane was treated along with 2% NaHCO₃ for 30 min at 80 °C to remove the trace amount of sulphides, followed by treatment with 10 mM of EDTA under constant conditions to get rid of any heavy metals and eventually with deionized water to freed the membrane from glycerine. The treated membrane was then mounted in clips and placed in diffusion cells. Dialysis membrane acting as donor compartment was placed with suspension of ZMD and its cocrystal materials. The drug and/or cocrystal solution was then allowed to stir at about 80 rpm (at 25 °C), followed by diffusion through the membrane towards the receptor compartment filled with 150 mL phosphate-buffered saline (pH = 7.4). Similar procedure was followed for permeation at solution with pH 1.2. Amount of substance released towards the receptor compartment through the dialysis membrane was further

analyzed by UV-Vis spectrophotometer. As such about 3 mL of the sample was taken out from the receptor compartment at definite interval of time and added equal volume of solution to maintain the volume constant. During the process we do not observe any significant change in the pH of the buffered solution at receptor compartment.

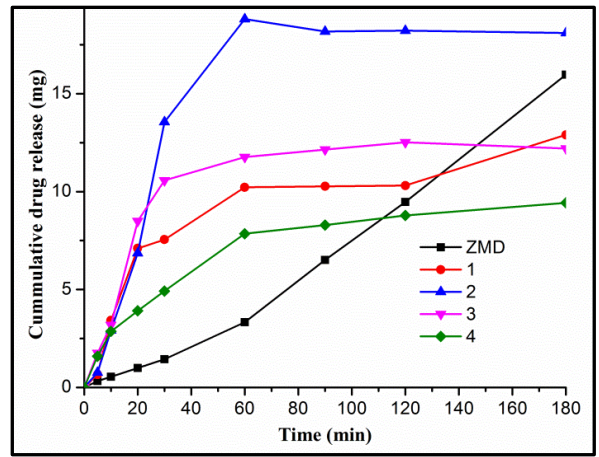
Table S8 Permeability rate % of ZMD and its cocrystals (**1** to **4**) at pH 1.2 and 7.4 for three set of experiments

Material	Time (min)	Permeability rate % at pH 1.2				Permeability rate % at pH 7.4			
		Set 1	Set 2	Set 3	Average	Set 1	Set 2	Set 3	Average
ZMD	5	0.481	0.470	0.480	0.477	1.616	1.593	1.602	1.603
	10	4.200	4.071	4.274	4.181	2.794	2.911	2.684	2.796
	20	12.666	12.660	12.497	12.607	4.950	4.950	4.792	4.897
	30	17.017	17.710	17.815	17.514	7.215	7.199	7.208	7.207
1	5	0.600	0.610	0.603	0.604	3.300	3.301	3.297	3.299
	10	6.361	6.576	6.012	6.316	17.128	16.017	17.256	16.800
	20	12.660	12.678	12.512	12.616	35.501	36.633	34.979	35.704
	30	18.611	17.985	18.626	18.407	37.758	37.084	37.793	37.545
2	5	11.967	12.110	11.890	11.989	3.841	3.792	3.897	3.843
	10	14.041	14.040	14.102	14.061	14.533	14.555	14.492	14.526
	20	20.014	19.897	19.904	19.938	34.136	33.982	34.293	34.137
	30	26.007	26.041	26.003	26.017	67.798	67.984	67.916	67.899
3	5	0.000	0.000	0.000	0.000	8.457	8.818	9.007	8.760
	10	0.197	0.216	0.220	0.211	15.953	16.106	15.870	15.976
	20	8.760	8.812	8.810	8.794	42.700	42.317	42.278	42.431
	30	20.513	20.501	20.510	20.508	52.893	52.850	52.850	52.864
4	5	6.122	6.000	6.218	6.113	8.001	7.843	7.899	7.914
	10	18.222	18.196	18.219	18.212	14.030	14.456	14.393	14.293
	20	28.070	28.076	28.006	28.050	19.553	19.451	19.553	19.519
	30	33.396	33.386	33.381	33.387	24.478	25.004	24.571	24.684

Fig. S10 Drug release at pH 1.2 (a) and 7.4 (b) at definite time period.

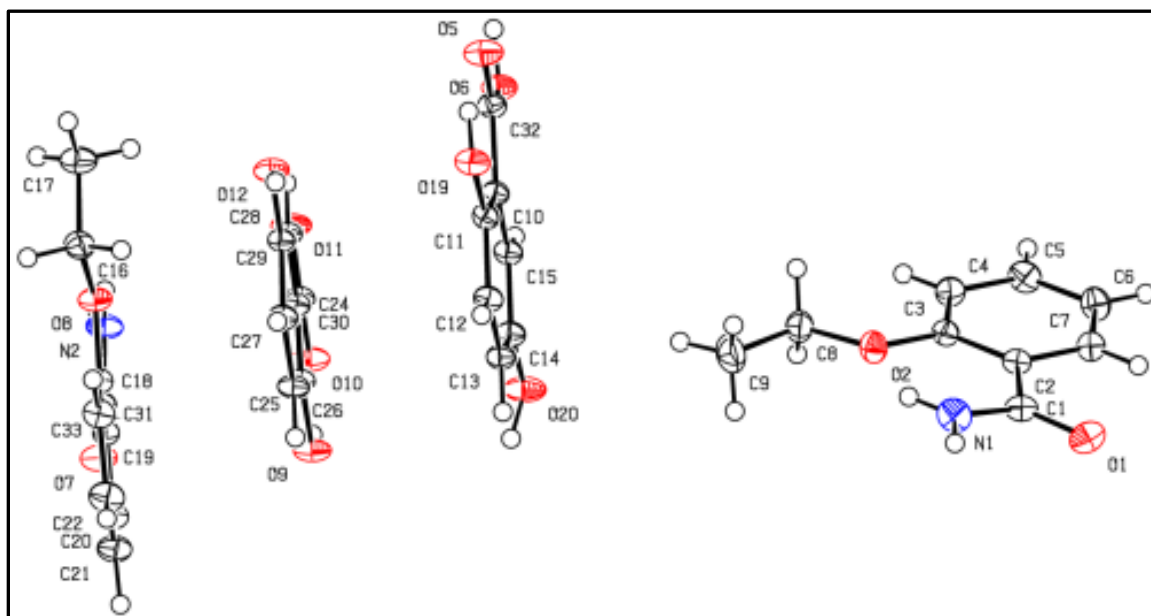


(a)

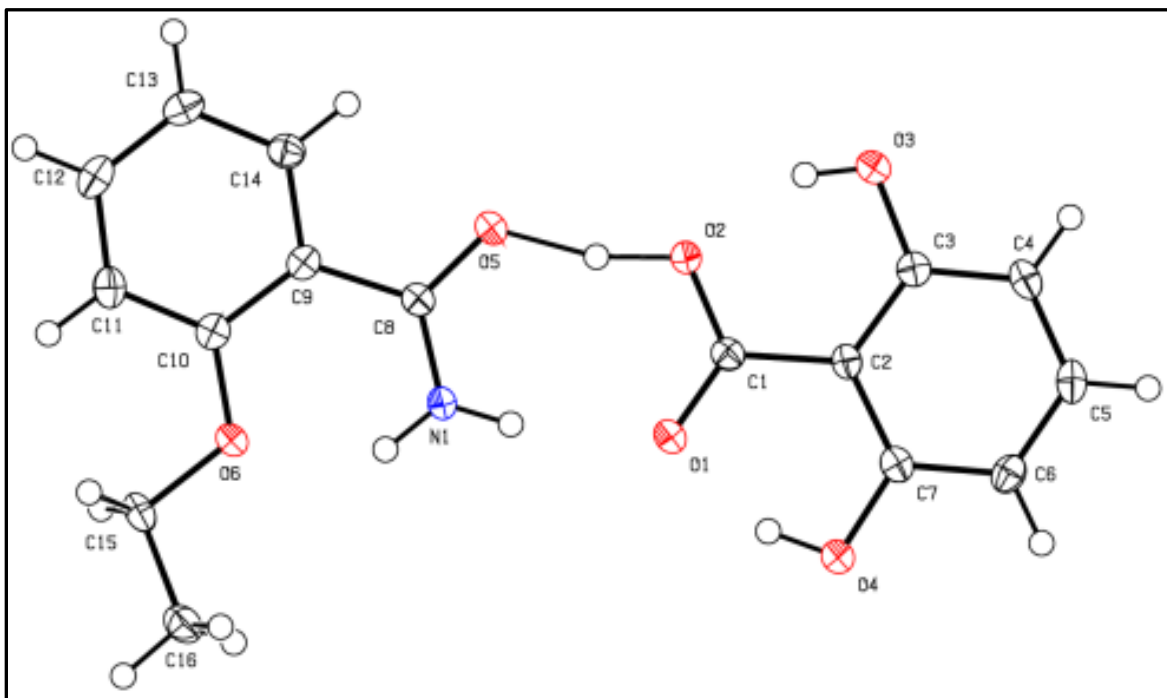


(b)

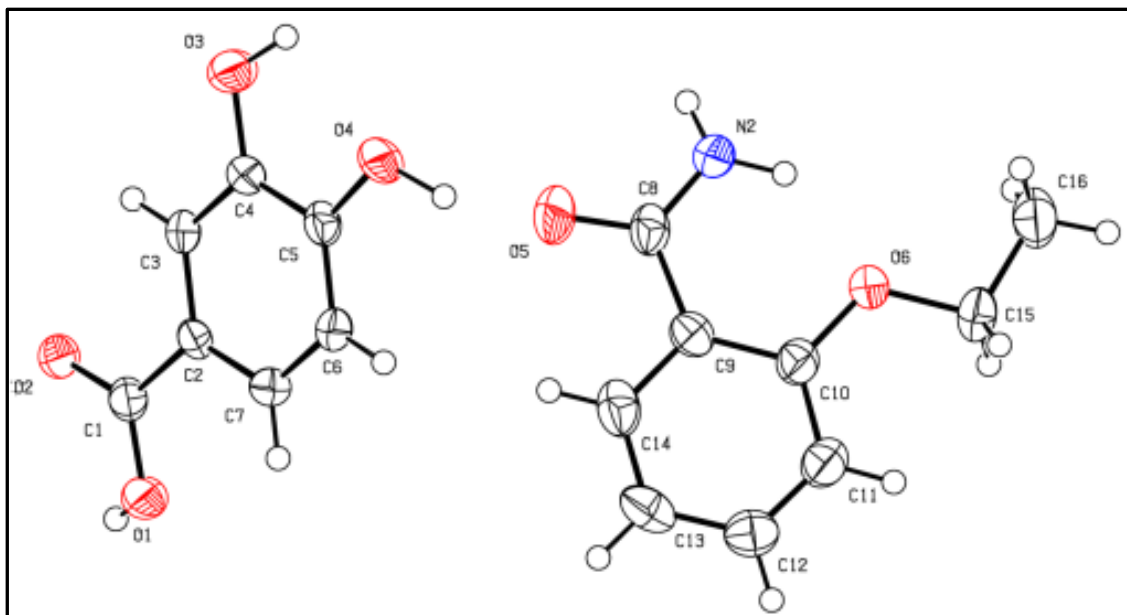
Fig. S11 ORTEP of cocrystals 1 to 4.



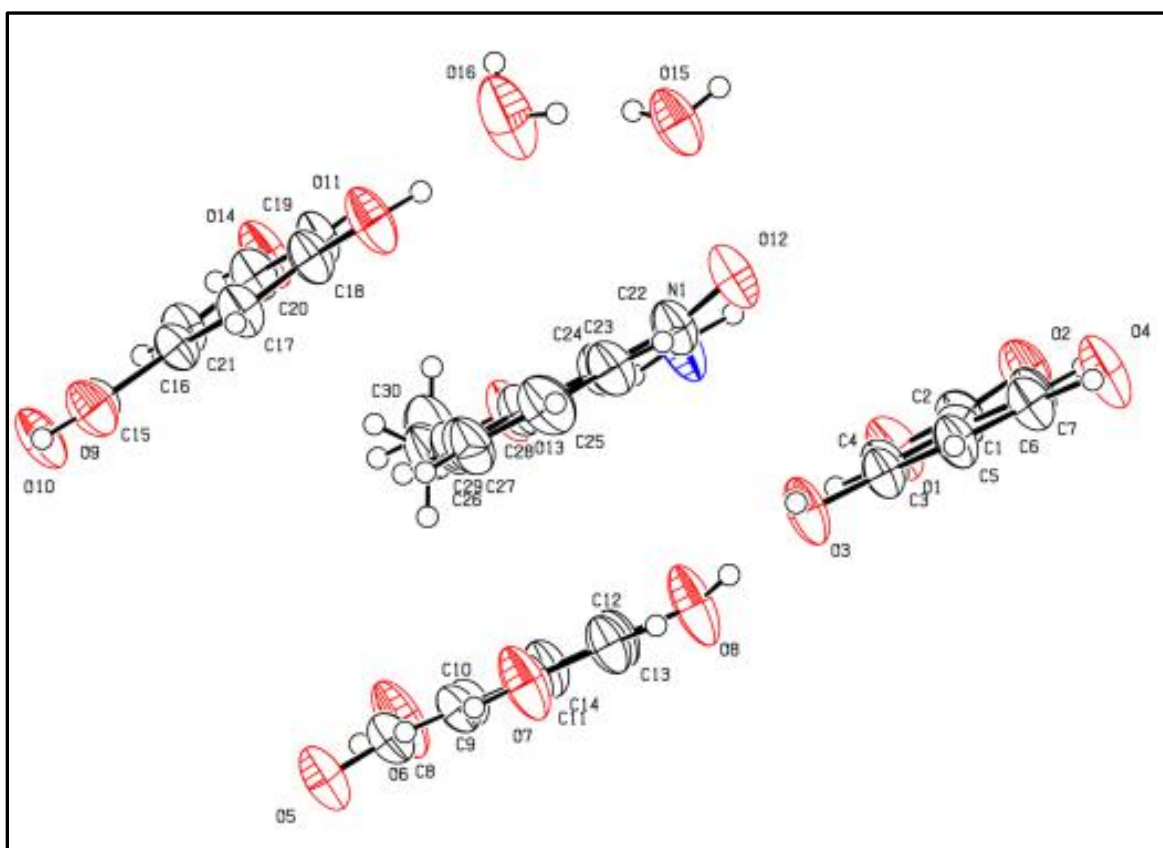
Cocystal 1



Cocystal 2



Cocystal 3



Cocystal 4